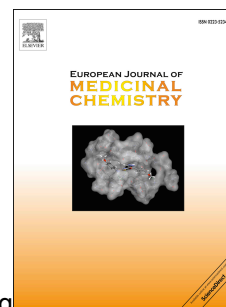


Accepted Manuscript

Identification of a potent 5-phenyl-thiazol-2-ylamine-based inhibitor of FLT3 with activity against drug resistance-conferring point mutations

Chiung-Tong Chen, John T.-A. Hsu, Wen-Hsing Lin, Cheng-Tai Lu, Shih-Chieh Yen, Tsu Hsu, Yu-Ling Huang, Jen-Shin Song, Chun-Hwa Chen, Ling-Hui Chou, Kuei-Jung Yen, Ching-Ping Chen, Po-Chu Kuo, Chen-Lung Huang, H. Eugene Liu, Yu-Sheng Chao, Teng-Kuang Yeh, Weir-Torn Jiaang



PII: S0223-5234(15)30034-9

DOI: [10.1016/j.ejmech.2015.05.008](https://doi.org/10.1016/j.ejmech.2015.05.008)

Reference: EJMECH 7887

To appear in: *European Journal of Medicinal Chemistry*

Received Date: 24 March 2015

Revised Date: 30 April 2015

Accepted Date: 5 May 2015

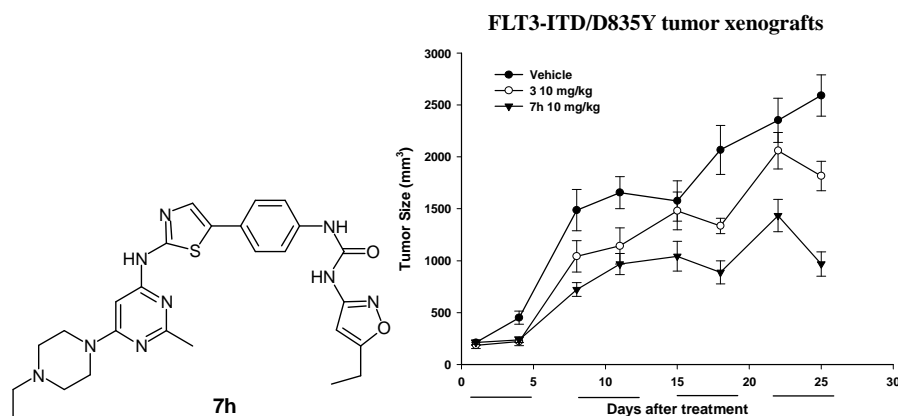
Please cite this article as: C.-T. Chen, J.T.-A. Hsu, W.-H. Lin, C.-T. Lu, S.-C. Yen, T. Hsu, Y.-L. Huang, J.-S. Song, C.-H. Chen, L.-H. Chou, K.-J. Yen, C.-P. Chen, P.-C. Kuo, C.-L. Huang, H. Eugene Liu, Y.-S. Chao, T.-K. Yeh, W.-T. Jiaang, Identification of a potent 5-phenyl-thiazol-2-ylamine-based inhibitor of FLT3 with activity against drug resistance-conferring point mutations, *European Journal of Medicinal Chemistry* (2015), doi: 10.1016/j.ejmech.2015.05.008.

This is a PDF file of an unedited manuscript that has been accepted for publication. As a service to our customers we are providing this early version of the manuscript. The manuscript will undergo copyediting, typesetting, and review of the resulting proof before it is published in its final form. Please note that during the production process errors may be discovered which could affect the content, and all legal disclaimers that apply to the journal pertain.

Graphical Abstract

Identification of a potent 5-phenyl-thiazol-2-ylamine-based inhibitor of FLT3 with activity against drug resistance-conferring point mutations

Chiung-Tong Chen, John T.-A. Hsu, Wen-Hsing Lin, Cheng-Tai Lu, Shih-Chieh Yen, Tsu Hsu, Yu-Ling Huang, Jen-Shin Song, Chun-Hwa Chen, Ling-Hui Chou, Kuei-Jung Yen, Ching-Ping Chen, Po-Chu Kuo, Chen-Lung Huang, H. Eugene Liu, Yu-Sheng Chao, Teng-Kuang Yeh, and Weir-Torn Jiaang



Identification of a potent 5-phenyl-thiazol-2-ylamine-based inhibitor of FLT3 with activity against drug resistance-conferring point mutations

Chiung-Tong Chen,^{1,#} John T.-A. Hsu,^{1,#} Wen-Hsing Lin,^{1,#} Cheng-Tai Lu,¹ Shih-Chieh Yen,¹ Tsu Hsu,¹ Yu-Ling Huang,¹ Jen-Shin Song,¹ Chun-Hwa Chen,¹ Ling-Hui Chou,¹ Kuei-Jung Yen,¹ Ching-Ping Chen,¹ Po-Chu Kuo,¹ Chen-Lung Huang,¹ H. Eugene Liu,² Yu-Sheng Chao,¹ Teng-Kuang Yeh,^{1,*} and Weir-Torn Jiaang^{1,*}

¹Institute of Biotechnology and Pharmaceutical Research, National Health Research Institutes, No. 35, Keyan Rd., Zhunan Town, Miaoli Country 350, Taiwan, R.O.C.

²Graduate Institute of Clinical Medicine, Taipei Medical University, Taipei, Taiwan, R.O.C.
Division of Hematology and Oncology, Department of Medicine, Wan Fang Hospital, Taipei Medical University, Taipei, Taiwan, R.O.C.

[#] Chiung-Tong Chen, John T.-A. Hsu and Wen-Hsing Lin contributed equally.

*Corresponding authors

Please send all correspondence to

Dr. Weir-Tong Jiaang (email: wtjiaang@nhri.org.tw)

Institute of Biotechnology and Pharmaceutical Research

National Health Research Institutes, Taiwan, R.O.C.

TEL: 886-37-246166 ext. 35712; FAX: 886-37-586456

Abstract

Numerous FLT3 inhibitors have been explored as a viable therapy for the treatment of acute myeloid leukemia (AML). However, clinical data have been underwhelming due to incomplete inhibition of FLT3 or the emergence of resistant mutations treated with these older

agents. We previously developed a series of 3-phenyl-1*H*-5-pyrazolylamine derivatives as highly potent and selective FLT3 inhibitors with good *in vivo* efficacy using an intravenous (IV) route. However, the poor bioavailability of these pyrazole compounds limits the development of these promising antileukemic compounds for clinical use. Herein, we describe a novel class of 5-phenyl-thiazol-2-ylamine compounds that are multi-targeted FLT3 inhibitors. From this class of compounds, compound **7h** was very potent against AML cell lines and exhibited excellent oral efficacy in AML xenograft models. In addition, further studies demonstrated that compound **7h** exhibited potent *in vitro* and *in vivo* activities against clinically relevant AC220 (**3**)-resistant kinase domain mutants of FLT3-ITD.

Keywords: FLT3 inhibitor; Acute myeloid leukemia; Receptor tyrosine kinase; ITD/D835Y; Xenograft model.

Abbreviations: FLT3, FMS-like Tyrosine Kinase-3; AML, acute myeloid leukemia; IV, intravenous; RTK, receptor tyrosine kinase; ITDs, internal tandem duplications; AL, activation loop; KD, kinase domain; TKIs, tyrosine-kinase inhibitors; SAR, structure-activity relationships; VEGFR2, vascular endothelial growth factor receptor 2; CSF1R, macrophage-colony stimulating factor receptor; PDGFR, platelet-derived growth factor receptor; RET, proto-oncogene tyrosine-protein kinase receptor; ALL, acute lymphoblastic leukemia; CML, chronic myelogenous leukemia; CR, complete regression; SC, subcutaneous; PO, per oral.

1. Introduction

Acute myeloid leukemia (AML) is an aggressive disease in which the rapid growth of abnormal leukemic cells in bone marrow inhibits the production of normal blood cells. Despite the success of conventional chemotherapy, the rate of relapse among AML patients is relatively high. The failure of the initial chemotherapy treatment and the refractory nature of AML have been associated with mutations that activate signal transduction pathways, resulting in enhanced proliferation and survival of leukemia cells [1,2]. The FMS-like tyrosine kinase-3 (FLT3) is a member of the class III membrane-bound receptor tyrosine kinase (RTK) family, along with c-KIT, FMS, and PDGFR [3,4]. The most frequent mutations among AML are FLT3 mutations, which account for approximately 30% of the genetic mutations that are predictive markers for a poor prognosis [4-6]. These mutations are typically internal tandem duplications (ITDs) in the juxtamembrane domain of the receptor and the missense point, or short-length mutations in the activation loop (AL) of the tyrosine kinase domain (KD) [7-9]. In addition to mutant forms of FLT3, wt-FLT3 is highly expressed in most cases of acute leukemia, and FLT3 over-expression is an unfavorable prognostic factor for overall survival with AML. In addition, over-expressed wt-FLT3 has the same sensitivity to FLT3 inhibitors as the FLT3/ITD mutants [10,11].

Due to the prevalence and refractory nature of the FLT3 mutations as well as the poor prognosis for those affected by it, numerous agents have been developed to directly inhibit wild-type and mutant FLT3. Several of these agents, such as midostaurin (PKC412, **1**) [12],

sorafenib (**2**) [13] and quizartinib (AC220, **3**) [14] (Figure 1), have been investigated as potential agents for the treatment of AML [15]. However, clinical responses to several of the early multi-targeted agents, such as lestaurtinib and **1**, have been underwhelming with limited reduction in bone marrow blasts and weak short-term responses. These underwhelming results may be primarily due to low potency and/or inadequate toleration of the inhibitors at effective doses, which result in failure to achieve complete and sustained inhibition of FLT3 in the patients' leukemic blast cells [15]. Newer, more potent and selective FLT3 inhibitors, such as **2** and **3**, possess the ability to achieve more sustained *in vivo* inhibition of FLT3 and have exhibited highly promising activity in early clinical studies [16]. Nevertheless, K. W. Pratz et al. reported that the inhibition of FLT3 autophosphorylation in a FLT3/ITD specimen does not always induce cell death, suggesting that some FLT3/ITD AML may not be addicted to FLT3 signaling. In addition, the response rate for diagnostic specimens is clearly higher for the least selective of the drugs due to the cytotoxic effect. These results indicate the potential therapeutic use of FLT3 inhibitors in patients with newly diagnosed FLT3-mutant AML might be less likely to respond clinically to highly selective FLT3inhibition [17].

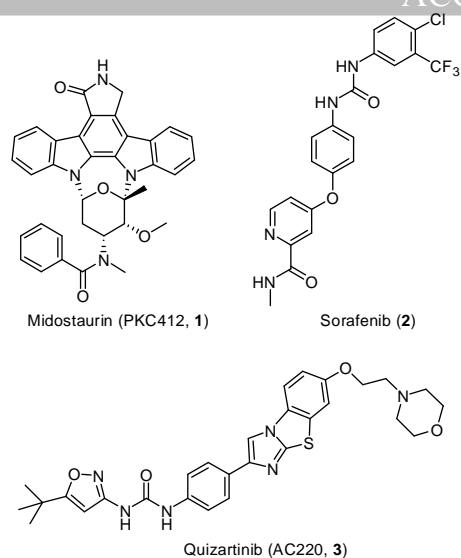


Figure 1. Structures of FLT3 inhibitors in the clinic.

Another significant result was that patients achieving a response to **3** often developed resistance-conferring point mutations (i.e., most commonly at D835 and less frequently at a “gatekeeper” residue, phenylalanine 691 (F691)) [18,19]. In addition, the emergence of resistant mutations has been reported in relapsed AML patients with FLT3-ITD treated with **1** [20] and **2** [21,22]. These clinical results suggest that secondary mutations conferring resistance were clinically problematic, which has spurred the development of new tyrosine-kinase inhibitors (TKIs) with activity against drug-resistant FLT3-ITD mutations [23].

Using structure-based design, we previously developed a novel class of 3-phenyl-1*H*-5-pyrazolylamine derivatives (Figure 2) as a versatile template for the development of specific kinase inhibitors and successfully identified a sulfonamide-substituted series of benzamides (Structure **I**) that inhibit both FLT3 and cellular proliferation [24,25]. Using rational design, we identified a second sulfonamide-substituted

series of pyrimidines (Structure **L**) [25] and two carbamate-substituted series of benzamides and pyrimidines (Structures **J** and **M**, respectively) [26] as potent inhibitors of FLT3. Recently, we developed another series of 3-phenyl-1*H*-5-pyrazolylamine-based inhibitors capable of greater inhibition of *in vitro* AML MOLM-13 cell growth and with a prolonged duration of *in vivo* action. In the previous study, two urea-substituted series of benzamides (Structure **K**) and pyrimidines (Structure **N**) were reported (Figure 2) [27,28]. However, these pyrazolylamine-based inhibitors were not orally active and exhibited moderate inhibitory activity toward drug-resistant FLT3-ITD mutations [24,28]. Both drawbacks could limit the future development of this pyrazole class of inhibitors for the treatment of AML patients in clinical trials.

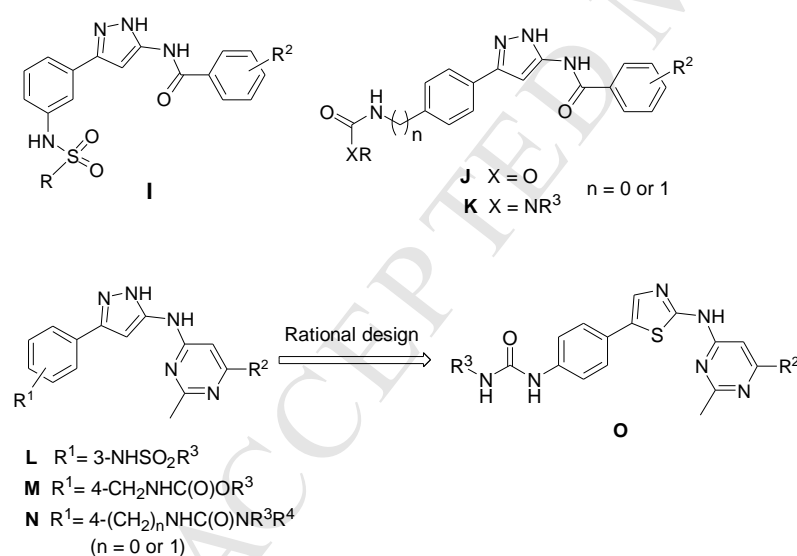


Figure 2. Identification of 5-phenyl-thiazol-2-ylamine derivatives as FLT3 inhibitors.

We supposed that little or no oral absorption for this class of pyrazole compounds may be due to the presence of more hydrogen-bond donors in the molecules. To continue to develop potent and orally active FLT3 inhibitors, we rationally designed a second class of

5-phenyl-thiazol-2-ylamine-based inhibitors (Structure **O**, Figure 2). The approach can remove a hydrogen-bond donor in the pyrazole ring. In this study, the structure-activity relationships (SAR), *in vitro* properties and pharmacokinetics of a series of pyrimidine derivatives are reported. This study has led to the discovery of urea **7h**, which is a multi-targeted kinase inhibitor with significant *in vitro* potency and *in vivo* efficacy against FLT3-ITD-expressing MOLM-13 and MV4;11 cell lines and FLT3-ITD/D835Y-expressing 32D cell line [29]. These promising results demonstrate the potential of **7h** as a drug candidate for further preclinical and clinical development.

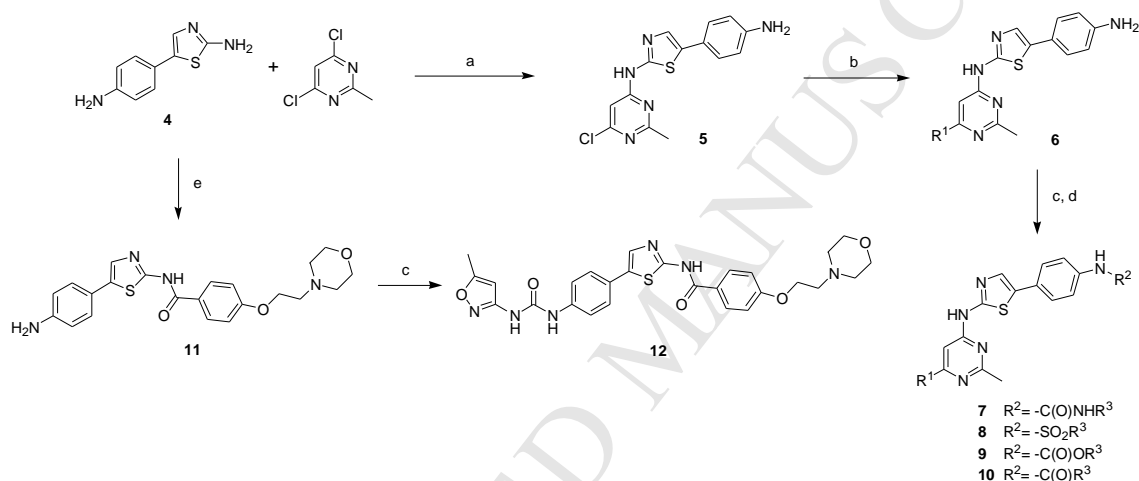
2. Results and discussion

2.1. Chemistry

The general synthetic route to 5-phenyl-thiazol-2-ylamine pyrimidines **7-10** (Table 1) is shown in Scheme 1. The synthesis began with the preparation of 5-phenyl-thiazol-2-ylamine **4** according to a previously published protocol [30]. Treatment of 5-phenyl-thiazol-2-ylamine **4** with 4,6-dichloropyrimidine in the presence of NaH and THF at 0 °C afforded 4-monosubstituted pyrimidine derivatives **5**. The treatment of these derivatives with 2° amines in pyridine at 80 °C yielded 4,6-disubstituted pyrimidines **6**, which were coupled with phenyl isocyanates (or heteroaryl carbamic acid 4-nitro-phenyl esters), benzenesulfonyl chloride, benzyl chloroformate, or benzoyl chloride to afford the final pyrimidine ureas **7** (except for Boc-**7b**, -**7d** and -**7i**), sulfonamide **8**, carbamate **9** or benzoyl **10**, respectively. Deprotection of

Boc-7 using TFA yielded final products **7b**, **7d** and **7i**.

The synthetic route to 5-phenyl-thiazol-2-ylamine benzamide **12** (Table 1) is shown in Scheme 1. The benzoyl chloride derivative with a water-solubilizing substituent was prepared according to a modified literature procedure [31]. The benzoyl chloride with a morphine group was employed to acylate amine **4** in pyridine to yield amide **11**. Intermediate **11** was coupled with (5-methyl-isoxazol-3-yl)-carbamic acid 4-nitro-phenyl ester to afford urea **12**.



Scheme 1. Reagents and conditions: (a) NaH, THF, 0 °C; (b) 2° amines, pyridine, 80 °C; (c) pyridine, phenyl isocyanate or (5-alkyl-isoxazol-3-yl)-carbamic acid 4-nitro-phenyl ester for **7** or **12**, benzenesulfonyl chloride for **8**, benzyl chloroformate for **9**, benzoyl chloride for **10**, rt; (d) CF₃COOH, rt for **7b**, **7d** and **7i**; (e) pyridine, benzoyl chloride with a morphine group, rt.

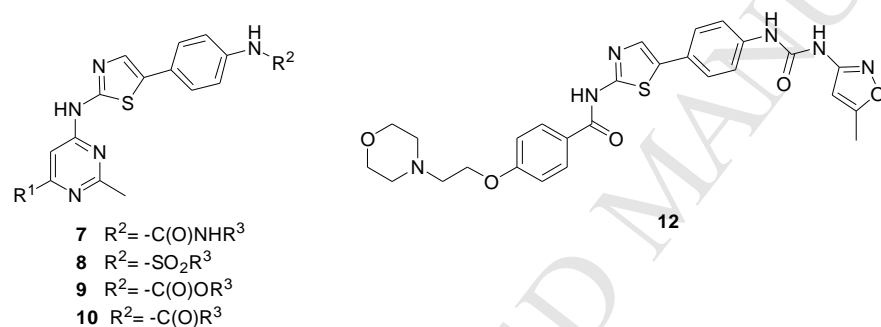
2.2. In vitro pharmacology and rat oral exposure assay

As shown in Table 1, the target compounds were tested against FLT3, vascular endothelial growth factor receptor 2 (VEGFR2), and Aurora A kinase (in-house kinases assays).

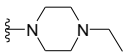
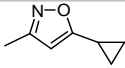
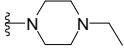
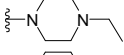
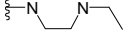
In addition, these compounds were further evaluated against the mutant FLT3 AML cell line MOLM-13 and oral exposure in rats. The first compound **7a**, which had a 4-methylpiperazine at R¹ and a phenyl substituent at R², moderately inhibited FLT3 (IC₅₀ = 0.079 μM) and

VEGFR2 ($IC_{50} = 0.16 \mu M$) but not Aurora A ($IC_{50} > 10 \mu M$). Lead **7a** potently inhibited the growth of MOLM-13 cells ($GI_{50} = 0.024 \mu M$) but suffered from undetectable drug levels in rat plasma after oral dosing (10 mg/kg). Conserving the phenyl urea moiety, hydrogen (**7b**), *para*-chlorination (**7c**) and *meta*-chlorination (**7d**) bearing different water-solubilizing substituents increased the inhibitory activity against VEGFR2 ($IC_{50} = 0.031$ to $0.053 \mu M$) and Aurora A ($IC_{50} = 0.095$ to $0.27 \mu M$) but resulted in no improvement in the oral absorption of the compounds.

Table 1. Inhibition of enzymes and cell proliferation with thiazole analogues.



Compd	R^1	R^3	$IC_{50} (\mu M)^*$			$GI_{50} (\mu M)$	Rats, PO 10 mg/kg $AUC_{(0-inf)}$ ng/mL *hr
			wt-FLT3	VEGFR2	Aurora A		
7a		$-C_6H_5$	0.079	0.16	>10	0.024	undetectable
7b		$-C_6H_5$	0.073	0.053	0.15	0.016	undetectable
7c		$4-Cl-C_6H_5-$	0.32	0.043	0.095	0.009	undetectable
7d		$3-Cl-C_6H_5-$	0.020	0.031	0.27	0.024	undetectable
7e			0.010	0.015	0.056	0.001	313
7f			0.049	0.01	0.041	0.003	632
7g			0.022	0.055	0.038	0.014	—
7h			0.038	0.025	0.032	0.002	1075
7i			0.014	0.007	0.038	0.003	undetectable

7j			0.033	0.015	0.036	0.002	—
8		-C ₆ H ₅	0.52	0.17	0.043	0.14	—
9		-CH ₂ C ₆ H ₅	0.083	0.12	0.32	0.003	66
10		-C ₆ H ₅	0.85	>1.0	0.14	0.019	—
12			0.58	0.37	0.025	0.21	—
1			0.037	0.25	0.080	0.055	—
2			0.044	0.042	3.8	0.056	—
3			0.069	0.43	>10	0.004	—

* IC₅₀ and GI₅₀ values are the means of at least two independent experiments.

Compounds **7a-d**, which contain a phenyl ring at R², exhibit potent inhibition against AML cell line MOLM-13. However, these compounds are not comparable to FLT3 inhibitor **3** (MOLM-13 GI₅₀ = 4 nM) and cannot be orally absorbed. To overcome these problems, the R² substituent of **7a** was changed from a phenyl group to a 5-alkyl-isoxazole group. According to the previous results from the development of 3-phenyl-1*H*-5-pyrazolylamine-based inhibitors, the terminal isoxazole ring of the urea maintains or increases the potency in enzymatic and cellular assays and improves the drug-like physical properties, such as solubility and lipophilicity (calculated LogP and CLogP) compared to the terminal phenyl ring of the urea.²⁷ As expected, 5-methyl-isoxazole **7e** increased the inhibitory activity against wt-FLT3 (IC₅₀ = 0.010), VEGFR2 (IC₅₀ = 0.015), Aurora A (IC₅₀ = 0.056) and MOLM-13 cells (GI₅₀ = 0.001 μM) and exhibited a considerable increase in oral exposure and oral bioavailability (F% =10). 5-Ethyl-isoxazole **7f** was 5 times less potent against FLT3 (IC₅₀ = 0.049 μM) but maintained its potency against VEGFR2 and Aurora A kinases relative to 5-methyl-isoxazole **7e**. In

addition, inhibitor **7f** potently inhibited the growth of MOLM-13 cells ($IC_{50} = 0.003 \mu M$) and had a positive effect on the pharmacokinetic profile ($F\% = 18$). The bulky 5-*tert*-butyl-isoxazole (**7g**) had a detrimental effect on the MOLM-13 inhibitory potency ($GI_{50} = 0.014 \mu M$) compared to methyl analogue **7e** and ethyl analogue **7f**.

Next, we examined the effects of water-solubilizing substituents on the 4-position of the pyrimidine ring and compared the potencies of compounds **7h-i** with *N*-methylpiperazine analogue **7f**. *N*-ethylpiperazine **7h** exhibited a potency that was similar to *N*-methylpiperazine **7f** in the enzymatic and cellular assays with slight improvements in the oral exposure and $F\% = 20$. In contrast, **7i** bearing a primary pyrrolidin-3-ylamine group produced extremely low circulating plasma levels but maintained its potency in the enzymatic and cellular assays. The hydrogen-bond donor number may partially account for the difference in the oral absorption between *N*-ethylpiperazine **7h** and pyrrolidin-3-ylamine **7i**. Although the more bulky 5-cyclopropyl-isoxazole **7j** was approximately as potent as 5-ethyl-isoxazole group **7h** in all of the *in vitro* assays, the preliminary toxicity study in mice indicated that compound **7j** was more toxic than **7h**. Therefore, the pharmacokinetic profile of **7j** was not further studied in rats. The preliminary toxicity study for compound testing was performed as previously described.²⁷

Previous studies indicated that the 3-phenyl-1*H*-5-pyrazolylamine-based sulfonamide-substituted series of pyrimidines (Structure **L**) and the carbamate-substituted series of pyrimidines (Structure **M**) were potent and selective FLT3 inhibitors (Figure 2).^{25,26}

An extensive SAR study was carried out by replacing the urea moiety of **7** with phenyl-substituted sulfonamide, carbamate and amide moieties to yield analogues **8**, **9** and **10**, respectively. Sulfonamide **8** was significantly less potent against the FLT3 and MOLM-13 cells as well as Aurora A ($IC_{50} = 0.043 \mu M$). Carbamate **9** exhibited only moderate inhibition of FLT3, VEGFR2 and Aurora A kinases ($IC_{50} = 0.083$ to $0.32 \mu M$) and suffered from low oral exposure in rats. However, **9** still exhibited a GI_{50} value of $0.003 \mu M$ against MOLM-13 cells. Amide **10** moderately inhibited Aurora A, weakly inhibited FLT3 and VEGFR2 ($IC_{50} > 0.80 \mu M$), and potently inhibited MOLM-13 cell growth ($GI_{50} = 0.019 \mu M$). The ability of **8** and **10** to inhibit the growth of MOLM-13 cells was not comparable to FLT3 inhibitor **3**. Therefore, the pharmacokinetic profiles of these compounds were not determined.

After optimizing the urea-substituted series of pyrimidines (compounds **7**, Structure **O**), we investigated the effect of the urea-substituted series of benzamides. Benzamide **12** effectively inhibited Aurora A ($IC_{50} = 0.025 \mu M$) but not FLT3, VEGFR2 and MOLM-13 cell growth. Therefore, further modification of lead **12** was not carried out. In comparison to FLT3 inhibitors **1**, **2** and **3**, which are currently in clinical development (Table 1), the inhibition of FLT3-mutant MOLM-13 cell growth by some of the potent urea compounds (**7**) is comparable to **3** ($GI_{50} = 4 nM$) and greater than **1** and **3** ($GI_{50} = 55$ and $56 nM$, respectively). Among these potent compounds (**7**), compound **7h** exhibited better oral exposure and oral bioavailability in rats, and therefore, this compound was chosen for more extensive *in vitro* and *in vivo* pharmacokinetic and antitumor efficacy studies.

2.3. Kinase inhibition profiles of **7h**

To better understand the enzyme inhibition by the potent compound, **7h** was assayed against 73 protein kinases covering the major oncogenic kinases of the human protein kinome at a concentration of 0.1 μ M. As shown in Table 2, **7h** inhibited 28 kinases by more than 50% at 0.1 μ M out of a panel of 73 tested kinases. Among these kinases, 18 kinases were potently inhibited by more than 80% including FLT3 (98%), PDGFR α (98%), SRC (97%), LYN A (96%), Aurora A (96%), RET (95%), CSF1R (94%), LCK (92%), and PDGFR β (91%). Therefore, this kinase inhibition profile indicated that compound **7h** is a multi-targeted kinase inhibitor that inhibits certain receptor tyrosine kinases, which include Aurora kinase A and B, macrophage-colony stimulating factor receptor (CSF1R), FMS-like tyrosine kinase-3 (FLT3), platelet-derived growth factor receptors (PDGFR α and PDGFR β), proto-oncogene tyrosine-protein kinase receptor (RET), Src-family non-receptor tyrosine kinases and the receptors of vascular endothelial growth factor (VEGFR type 2 and 3).

Table 2. Kinase inhibition profile of compounds **7h**.

Kinase	0.1 μ M % inhibition	Kinase	0.1 μ M % inhibition
FLT3	98	VEGFR2	85
PDGFR α	98	AURKB	85
SRC	97	TRKA	82
LYN A	96	VEGFR3	80
AURKA	96	BLK	78
RET	95	YES1	72
CSF1R	94	ABL1	66
LCK	92	RET V804L	65

PDGFR β	91	KIT	64
RET		PDGFR α	
V804L	89	V561D	63
FGR	89	MEK1	62
LYN B	88	IRAK4	61
FLT3		Tie2	
D835Y	87		61
RET		ABL1	
Y791F	86	T315I	51

2.4. Antiproliferative effects of **7h** on leukemia cell lines

The activity of **7h** was evaluated in a panel of leukemic cell lines (Table 3). Potent anti-proliferative activity of **7h** was observed in FLT3-driven MOLM-13 and MV4;11 AML cell lines containing the FLT-ITD-activating mutation. The IC₅₀ values of **7h** for the MOLM-13 and MV4;11 cells were 0.002 and 0.001 nM, respectively. Compound **7h** was weakly cytotoxic against U937 human leukemic monocyte lymphoma cells (not expressing FLT3) [32] (GI₅₀ = 1.1 μ M). In contrast, the IC₅₀ values for the inhibition of RS4;11 AML cells (expressing native FLT3) [33] and K562 human chronic myeloid leukemia cells (expressing wt-BCR/ABL) [11] were between 0.1 and 0.2 μ M. Among the FLT3 inhibitors shown in Table 3, the growth inhibitory activity of **7h** against the MOLM-13 and MV4;11 AML cell lines was comparable to that of **3**, which is a specific FLT3 inhibitor. Multi-targeted kinase inhibitors **1** and **7h** appeared to induce higher growth inhibition against U937 and RS4;11.

Table 3. Inhibition of leukemia cell growth by **7h** and **1-3**.

Cell line*	Characterization	GI ₅₀ (μ M)			
		7h	1	2	3
MOLM-13	AML-FLT3-ITD (heterozygous)	0.002	0.055	0.056	0.004

MV4;11	AML-FLT3-ITD (homozygous)	0.001	0.038	0.043	0.003
U937	AML-FLT3-negative	1.1	1.4	3.4	>20
RS4;11	ALL-wt-FLT3 (homozygous)	0.11	0.40	9.3	2.2
K562	CML-Bcr-Abl FLT3-negative	0.19	>20	7.3	>20

*AML, acute myelocytic leukemia; ALL, acute lymphoblastic leukemia; CML, chronic myelogenous leukemia

2.5 *In vitro* activity of **7h** against clinically relevant drug resistance caused by FLT3-ITD KD mutants

Due to its promising potency toward the FLT3-driven AML cell lines, the activity of **7h** against four different KD mutants of FLT3-ITD, which confer resistance to **3** [20-23]. In this study, we first examined the cellular GI₅₀ values of **3** and **7h** against 32D cells expressing FLT3-ITD and its KD mutants D835V/Y/F and F691L [29]. As shown in Table 4, compounds **3** and **7h** potently inhibited proliferation of native FLT3-ITD with a GI₅₀ value of 10 pM. The cell proliferation-based assays indicated that the sensitivity toward **7h** differed significantly for inhibiting FLT3-ITD D835Y (GI₅₀ = 0.006 μM), D835V (GI₅₀ = 0.004 μM), D835F (GI₅₀ = 0.038 μM) and F691L (GI₅₀ = 0.071 μM). These results are similar to the sensitivity profiles of **3** against FLT3-ITD D835Y/V/F and F691L, which exhibited GI₅₀ values of 0.016, 0.027, 0.15 and 0.22 μM, respectively, for the four mutants. Along with the results from Table 4, **7h** exhibits very potent *in vitro* growth inhibitory effects (GI₅₀ < 10 nM) against FLT3-ITD D835Y/V and is 3- to 6-fold more potent than **3** at inhibiting proliferation of these FLT3-ITD mutants, as shown in Table 4.

Table 4. Activity of **3** and **7h** against 32D cells expressing native and drug-resistant mutants of FLT3-ITD.

Cell line	GI ₅₀ (μM)*	
	7h	3

ITD alone	0.00001	0.00001
ITD-D835Y	0.006	0.016
ITD-D835V	0.004	0.027
ITD-D835F	0.038	0.15
ITD-F691L	0.070	0.22

*GI₅₀ values are the means of three independent experiments.

Because inhibitor of **7h** exhibits cytotoxicity in 32D cells expressing FLT3-ITD KD mutants, it was important to verify that the mechanism of cell death was directly linked to the inhibition of FLT3. Next, we analyzed the activity of **7h** against wild-type, ITD, ITD D835Y or F691L mutants of FLT3 in a biochemical assay for the phosphorylation of FLT3 (Figure 3). A western blot was performed using HEK293T cells engineered to express FLT3-ITD/D835Y or FLT3-ITD/F691L [27]. According to the cell-based proliferation assay, the phosphorylation of all of the FLT3-WT, FLT3-ITD, FLT3-ITD/D835 and FLT3-ITD/F691L was inhibited by compound **7h** with IC₅₀ values of approximately 10 nM.

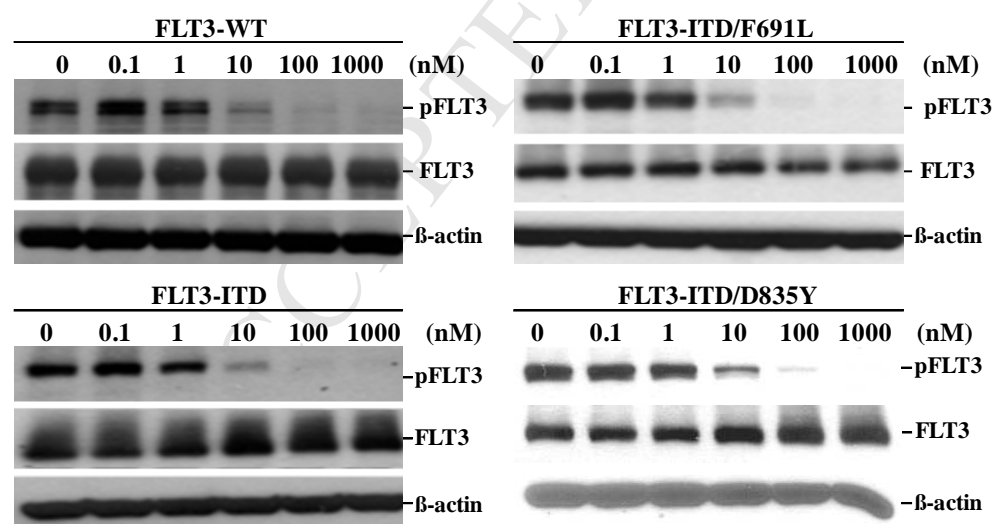


Figure 3. HEK293T cells engineered to express FLT3-WT, FLT3-ITD, FLT3-ITD/D835Y or FLT3-ITD/F691L were analyzed. The HEK293T-FLT3 cells were treated with compound **7h** at various concentrations for 1 hr, and the FLT3 ligand (50 ng/mL) was added for 5 min to prepare the cell lysate for detection of changes in FLT3 phosphorylation by western blot analysis.

2.6. Pharmacokinetic and in vivo efficacy studies of **7h**

Table 5 shows the PK data obtained from the evaluation of **7h** in male Sprague–Dawley rats and ICR mice. In both species, **7h** exhibited high volumes of distribution ($V_{ss} = 8.2$ L/kg in rats and 21 L/kg in mice) and plasma clearances ($CL = 31.6$ mL/min/kg in rats and 82 mL/min/kg in mice) after intravenous (IV, 2 mg/kg) administration. 10 mg/kg was orally administered as a solution containing 22% hydroxypropyl- β -cyclodextrin in water and absorbed with a moderate half-life ($t_{1/2} = 4.3$ hr) in rats and a shorter half-life ($t_{1/2} = 1.8$ hr) in mice. Both the C_{max} (122 ng/mL) and AUC (1075 ng/mL*hr) in rats were similar to those in mice, and the oral bioavailability ranged from 20% in rats to 35% in mice. With favorable pharmacokinetic properties and excellent cellular potency against AML cell lines, **7h** was appropriate for continued investigation in *in vivo* studies including the MV4;11 tumor xenograft model, MOLM-13 myeloproliferative mouse model and FLT3-ITD/D835Y tumor xenograft model (Figure 4).

Table 5. Pharmacokinetic profile of compound **7h**.

Species	IV (dose: 2 mg/kg)		PO (dose: 10 mg/kg)			
	CL (mL/min/kg)	V_{ss} (L/kg)	$T_{1/2}$ (hr)	C_{max} (ng/mL)	AUC _(0-inf) (ng/mL*hr)	F (%)
Rats	31.6	8.2	4.3	122	1,075	20
Mice	82	21	1.8	168	942	35

In a MV4;11 tumor xenograft model (Figure 4a), compound **7h** was administered orally at doses of 10 and 25 mg/kg qd on days 1-5 and 8-12. By the end of this period, the MV4;11 tumors reached an average volume of 200 mm³. At 10 or 25 mg/kg, the tumor growth was

inhibited for the first 5 days. After this period, complete disappearance of the tumor mass was observed after dosing was halted. Treatment with 10 or 25 mg/kg resulted in 6 of 7 and 7 of 7 treated animals with complete regression (CR), respectively, during the 48 days of post-treatment observation. Treatment with **3**, which is a clinically active FLT3 inhibitor, also exhibited substantial activity with a once daily oral dosing at 10 mg/kg, and complete regression was observed in 6 of the 7 treated animals, which comparable to the efficacy of **7h** at the same dose.

To determine whether **7h** is also efficacious in a MOLM-13 xenograft model, we used a myeloproliferative mouse model where the MOLM-13 cells were IV inoculated into SCID mice and allowed to proliferate for one day prior to treatment with either the vehicle, **3** or **7h** (Figure 4b). The median survival for the mice treated with the vehicle was 20 days. At a dose of 10 mg/kg once a day using **3** and **7h**, the median survival was extended to 33 and 29 days, respectively. The median survival in the group treated with **7h** at a daily dose of 25 mg/kg was extended to 38 days, which is an increase of 90% relative to the vehicle control and twice the percentage relative to treatment with **7h** at a low dose (Figure 4b). FLT3 inhibitor **3** exhibited better efficacy than **7h** in this animal model.

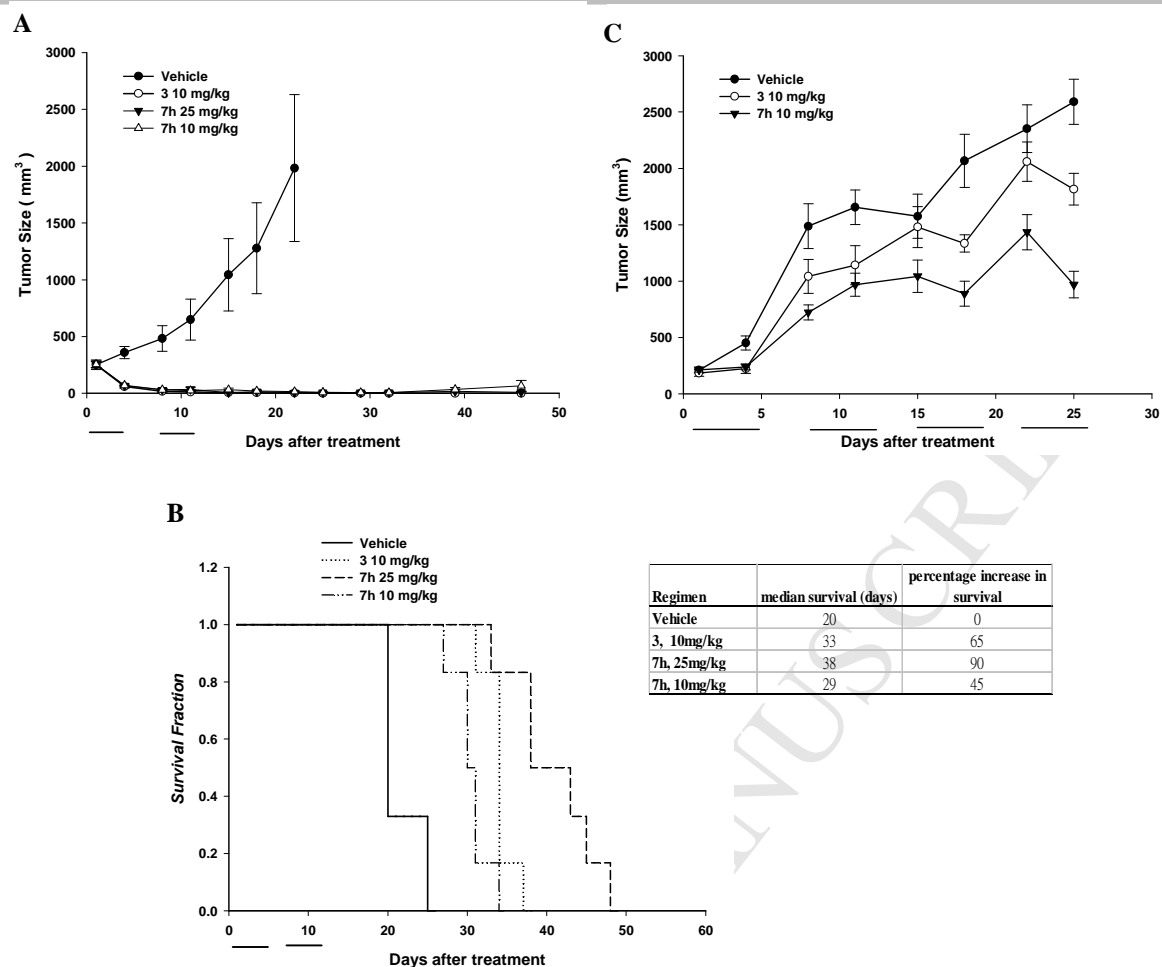


Figure 4. Comparison of antitumor efficacy of compounds **3** and **7h** in xenograft mouse models. (A) Human MV4;11 cells were implanted SC in nude mice. After the average size of the tumors reached to 200 mm³, mice were dosed with **3** or **7h** (qd, days 1-5 and 8-12) by oral gavage. The tumor size is expressed as the mean \pm SEM (n = 6-7/group). (B) MOLM-13 cells were IV inoculated into SCID mice. From the 2nd day after inoculation, mice were administered **7h** at 10 or 20 mg/kg or **3** at 10 mg/kg or vehicle (qd, days 2-5 and 8-12) by oral gavage (n = 6/group). (C) Mice were implanted subcutaneously (SC) with 32D/FLT3-ITD-D835Y cells. When the average tumor volume reached 200 mm³ in size, **3** or **7h** was administered orally at a dose of 10 mg/kg with a 5 days on/2 days off schedule for 4 weeks. The tumor size is expressed as the mean \pm SEM (n = 9/group).

Compound **7h** was very active against FLT3-ITD AL mutant D835Y in both the cell-based proliferation and biochemical assay for the phosphorylation of FLT3 (Table 4 and Figure 3). To determine if the *in vitro* effects of **7h** correlate with *in vivo* tumor growth inhibition, the efficacy of **7h** was examined against FLT3-ITD/D835Y tumor xenografts in

nude mice (Figure 4c). Mice were implanted subcutaneously (SC) with 32D/FLT3-ITD-D835Y tumor cells, and treatment with compound **3** or **7h** was initiated when tumors reached an average volume of 200 mm³. Compound **3** or **7h** was administered orally at a dose of 10 mg/kg with a 5 days on/2 days off schedule for 4 weeks. Compound **7h** exhibited a statistically significant TGI (68%) [34] in tumor-bearing mice treated with the drug compared with vehicle-treated control mice. However, treatment with **3** at the same dose did not yield a biologically significant TGI (32%). The drug-resistant xenograft model demonstrates that **7h** effectively reduced the tumor size with 4 weeks of treatment at an oral dose of 10 mg/kg/day. **7h** is well tolerated in mice at the effective dose.

3. Conclusion

A rational design approach successfully identified a potent and orally bioavailable compound (**7h**), which is a multi-targeted FLT3 inhibitor. In AML cells, **7h** exhibited similar *in vitro* potency and *in vivo* efficacy to known FLT3 inhibitor **3**. Importantly, **7h** appears to be highly active against clinically relevant FLT3-ITD AL mutations, especially at the D835 residue (D835Y/V), and demonstrates *in vivo* efficacy in the FLT3-ITD/D835Y xenograft model. These promising results indicate that **7h** could be an effective first-line TKI therapy in AML patients or second-line therapy for the treatment of clinical drug resistance.

4. Experimental

4.1. Chemistry

4.1.1. General methods

All commercial chemicals and solvents are reagent grade and were used without further treatment unless otherwise noted. ^1H NMR spectra were obtained with a Varian Mercury-300 or a Varian Mercury-400 spectrometer. Chemical shifts were recorded in parts per million (ppm, δ) and were reported relative to the solvent peak or TMS. LC/MS data were measured on an Agilent MSD-1100 ESI-MS/MS System. High-resolution mass spectra (HRMS) were measured with a Thermo Finnigan (TSQ Quantum) electrospray ionization (ESI) mass spectrometer. Flash column chromatography was done using silica gel (Merck Kieselgel 60, No. 9385, 230-400 mesh ASTM). Reactions were monitored by TLC using Merck 60 F₂₅₄ silica gel glass backed plates (5 × 10 cm); zones were detected visually under ultraviolet irradiation (254 nm) or by spraying with phosphomolybdic acid reagent (Aldrich) followed by heating at 80 °C. All starting materials and amines were commercially available unless otherwise indicated. The purity of compounds was determined by a Hitachi 2000 series HPLC system. Except for compound **12**, purity of target compounds **7**, **8**, **9** and **10** were over 95% based on reverse phase C₁₈ column (Agilent ZORBAX Eclipse XDB-C18 5 μm , 4.6 mm × 150 mm, Condition A) and reverse phase phenyl column (Waters XBridge Phenyl 5 μm , 4.6 mm × 150 mm, Condition B) under the following gradient elution condition: Mobile phase A-acetonitrile (10% to 90%, 0 to 45 min) and mobile phase B-10 mM NH₄OAc aqueous solution containing 0.1% formic acid (90% to 10%, 0 to 45 min). The flow-rate was 0.5

ml/min and the injection volume was 20 μ l. The system operated at 25 °C. Peaks were detected at λ = 254 nm.

4.1.2. *N*-[5-(4-aminophenyl)-1,3-thiazol-2-yl]-6-chloro-2-methylpyrimidin-4-amine (**5**)

To a solution of 5-(4-aminophenyl)-1,3-thiazol-2-amine **4** (1.0 equiv) and 4,6-dichloro-2-methylpyrimidine (1.0 equiv) in THF at 0 °C was added NaH (60% in oil, 2.0 equiv) and the resultant mixture was stirred at room temperature for 4 h. The reaction was cooled to 0°C and quenched with 2 N HCl to pH = 3. The mixture was partitioned between THF and saturated NaHCO₃ solution. The organic layer was separated, dried over MgSO₄ and concentrated in vacuo. Purification by flash column chromatography (eluted with CH₂Cl₂/EtOAc/THF) yielded **5**. ¹H NMR (300 MHz, DMSO-*d*₆): δ 11.77 (s, 1H), 7.54 (s, 1H), 7.28-7.24 (m, 2H), 6.89 (s, 1H), 6.59-6.56 (m, 2H), 5.31 (s, 2H), 2.55 (s, 3H); MS (ES⁺) *m/z* calcd. for C₁₄H₁₂ClN₅S: 317.05; found: 318.1 (M+H⁺).

4.1.3. General procedure for the preparation of compounds **6**

To a solution of **5** (1.0 equiv) in pyridine at room temperature was added 2° amines (2.0 equiv) and the resultant mixture was stirred at 80 °C for 2 h. After cooling to room temperature, the reaction mixture was evaporated to dryness and the residue suspended in saturated NaHCO₃ solution. The suspension was vigorously stirred at room temperature for 1 h and the resultant solid was collected by filtration. The crude product was used for the next step without further purification.

4.1.4. General procedure for the preparation of urea analogues **7**

To a solution of **6** (1.0 equiv) in pyridine at room temperature was added phenyl isocyanate (1.1 equiv) or (5-alkyl-isoxazol-3-yl)-carbamic acid 4-nitro-phenyl ester (1.5 equiv). After 2 h of stirring at room temperature, the reaction was worked up as described for compounds **6** to yield crude products **7**, *N*-Boc **7b**, *N*-Boc **7d** and *N*-Boc **7i**. The crude products **7** were further purified by recrystallization with CH₃CN/CH₃OH to yield **7**.

To a solution of *N*-Boc **7b** *N*-Boc **7d** or *N*-Boc **7i** (1.0 equiv) in CH₂Cl₂ at room temperature was added trifluoroacetic acid (10 equiv). After 0.5 h of stirring at room temperature, the reaction mixture was evaporated to dryness. The residue was suspended in saturated NaHCO₃ solution and the resulting suspension was vigorously stirred at room temperature for 1 h. The resultant solid was collected by filtration and recrystallized from CH₃CN/CH₃OH to yield **7b**, **7d** or **7i**.

4.1.4.1.

1-[4-(2-{[2-methyl-6-(4-methylpiperazin-1-yl)pyrimidin-4-yl]amino}-1,3-thiazol-5-yl)phenyl]-3-phenylurea (7a)

Mp 252–253 °C (HCl salt). ¹H NMR (300 MHz, DMSO-*d*₆): δ 11.11 (s, 1H), 8.77 (s, 1H), 8.67 (s, 1H), 7.64 (s, 1H), 7.49-7.44 (m, 6H), 7.28 (t, *J* = 7.8 Hz, 2H), 6.97 (t, *J* = 7.2 Hz, 1H), 6.05 (s, 1H), 3.50 (br s, 4H), 2.41-2.34 (m, 7H), 2.22 (s, 3H); ¹³C NMR (100 MHz, DMSO-*d*₆) δ 26.1, 43.9, 46.2, 54.6, 82.6, 118.7, 119.1, 122.3, 126.2, 126.3, 129.3, 130.7,

133.0, 139.2, 140.1, 152.9, 157.7, 158.5, 162.9, 165.6; MS (ES⁺) m/z calcd. for C₂₆H₂₈N₈OS: 500.63; found: 501.47 (M+H⁺); HRMS (ESI) calcd. for C₂₆H₂₉N₈OS: 501.2185; found: 501.2178 (M+H⁺); HPLC (condition A) *t*_R = 22.41 min, 99.5%, (condition B) *t*_R = 24.49 min, 99.1%.

4.1.4.2.

N-[4-(2-[6-(4-aminopiperidino)-2-methyl-4-pyrimidinyl]amino-1,3-thiazol-5-yl)phenyl]-*N'*-phenylurea (**7b**)

Mp 269–270 °C. ¹H NMR (400 MHz, DMSO-*d*₆): δ 8.80 (s, 1H), 8.70 (s, 1H), 7.64 (s, 1H), 7.49–7.45 (m, 6H), 7.28 (t, *J* = 7.6 Hz, 2H), 6.97 (t, *J* = 7.2 Hz, 1H), 6.06 (s, 1H), 4.12 (d, *J* = 12.0 Hz, 2H), 3.33 (br s, 2H, overlapping with water peak), 2.94 (t, *J* = 11.6 Hz, 4H), 2.41 (s, 3H), 1.76 (d, *J* = 10.0 Hz, 2H), 1.16 (d, *J* = 10.4 Hz, 2H); ¹³C NMR (100 MHz, DMSO-*d*₆) δ 19.1, 26.1, 32.3, 42.9, 56.5, 82.4, 118.7, 119.0, 122.1, 126.0, 126.2, 129.2, 130.7, 132.9, 139.5, 140.4, 153.1, 157.7, 158.5, 162.5, 165.7; HRMS (ESI) calcd. for C₂₆H₂₉N₈OS: 501.2185; found: 501.2184 (M+H⁺); HPLC (condition A) *t*_R = 21.51 min, 99.6%, (condition B) *t*_R = 23.57 min, 98.1%.

4.1.4.3.

N-(4-chlorophenyl)-*N'*-[4-(2-[6-(4-ethylpiperazino)-2-methyl-4-pyrimidinyl]amino-1,3-thiazol-5-yl)phenyl]urea (**7c**)

Mp 256–257 °C (HCl salt). ¹H NMR (300 MHz, DMSO-*d*₆): δ 11.10 (s, 1H), 8.84–8.81 (m, 2H), 7.63 (s, 1H), 7.49–7.43 (m, 6H), 7.32 (s, 1H), 7.29 (s, 1H), 6.03 (s, 1H), 3.48 (br s, 4H), 2.40–2.30 (m, 9H), 1.01 (t, *J* = 7.2 Hz, 3H); ¹³C NMR (75 MHz, DMSO-*d*₆) δ 12.4, 26.1,

44.0, 52.1, 52.4, 82.6, 110.0, 119.2, 120.2, 125.3, 125.8, 129.1, 130.6, 133.1, 139.0, 139.1, 152.8, 157.7, 158.6, 162.9, 165.6; MS (ES⁺) m/z calcd. for C₂₇H₂₉ClN₈OS: 548.19; found: 549.2 (M+H⁺); HRMS (ESI) calcd. for C₂₇H₃₀ClN₈OS: 549.1952; found: 549.1948 (M+H⁺); HPLC (condition A) *t*_R = 25.92 min, 97.4%, (condition B) *t*_R = 28.18 min, 97.5%.

4.1.4.4.

N-(3-chlorophenyl)-*N'*-(4-2-[(2-methyl-6-piperazino-4-pyrimidinyl)amino]-1,3-thiazol-5-ylphenyl)urea (**7d**)

Mp 345–346 °C. ¹H NMR (400 MHz, DMSO-*d*₆): δ 11.07 (s, 1H), 9.01 (s, 1H), 8.99 (s, 1H), 7.72–7.65 (m, 2H), 7.57–7.50 (m, 4H), 7.32–7.27 (m, 2H), 7.04–7.00 (m, 2H), 6.06 (s, 1H), 3.43 (br s, 4H, overlapping with water peak), 2.76 (t, *J* = 4.8 Hz, 4H), 2.41 (s, 3H); ¹³C NMR (100 MHz, DMSO-*d*₆) δ 26.1, 45.2, 45.7, 82.3, 117.1, 117.9, 119.2, 121.6, 125.4, 126.2, 130.7, 130.8, 133.0, 133.6, 139.3, 142.1, 153.0, 157.7, 158.5, 162.9, 165.6; MS (ES⁺) m/z calcd. for C₂₅H₂₅ClN₈OS: 520.16; found: 521.1 (M+H⁺); HRMS (ESI) calcd. for C₂₅H₂₆ClN₈OS: 521.1639; found: 521.1636 (M+H⁺); HPLC (condition A) *t*_R = 24.80 min, 97.6%, (condition B) *t*_R = 27.09 min, 99.0%.

4.1.4.5.

N-(5-methyl-3-isoxazolyl)-*N'*-[4-(2-[2-methyl-6-(4-methylpiperazino)-4-pyrimidinyl]amino)-1,3-thiazol-5-yl]phenyl]urea(**7e**)

Mp 344–345 °C. ¹H NMR (400 MHz, DMSO-*d*₆): δ 11.15 (s, 1H), 9.46 (s, 1H), 8.92 (s, 1H), 7.67 (s, 1H), 7.50 (ABq, Δ*v*_{AB} = 13.4 Hz, *J*_{AB} = 8.8 Hz, 4H), 6.55 (s, 1H), 6.04 (s, 1H), 3.50 (t, *J* = 4.8 Hz, 4H), 2.41 (s, 3H), 2.37 (m, 7H), 2.21 (s, 3H); ¹³C NMR (75 MHz, DMSO-*d*₆) δ 12.6, 26.0, 43.9, 46.2, 54.6, 82.6, 96.0, 119.5, 126.3, 126.9, 130.5, 133.3, 138.3, 151.7, 157.7, 158.6, 159.1, 162.9, 165.6, 169.7; MS (ES⁺) *m/z* calcd. for C₂₄H₂₇N₉O₂S: 505.20; found: 506.2 (M+H⁺); HRMS (ESI) calcd. for C₂₄H₂₈N₉O₂S: 506.2087; found: 506.2082 (M+H⁺); HPLC (condition A) *t*_R = 19.85 min, 100%, (condition B) *t*_R = 21.31 min, 98.3%.

4.1.4.6.

1-(5-ethyl-1,2-oxazol-3-yl)-3-[4-(2-{[2-methyl-6-(4-methylpiperazin-1-yl)pyrimidin-4-yl]amino}-1,3-thiazol-5-yl)phenyl]urea Diformate (7f)

Mp 326–327 °C. ¹H NMR (400 MHz, DMSO-*d*₆): δ 9.83 (s, 1H), 9.29 (s, 1H), 8.29 (s, 2H), 7.75 (s, 1H), 7.58 (s, 4H), 6.63 (s, 1H), 6.14 (s, 1H), 5.53 (br s, 1H), 3.59 (s, 4H), 2.79 (d, *J* = 6.0 Hz, 2H), 2.58 (s, 3H), 2.33 (s, 3H), 1.29 (s, 3H); ¹³C NMR (75 MHz, DMSO-*d*₆) δ 11.9, 20.2, 26.1, 43.9, 46.14, 54.6, 82.6, 94.7, 119.5, 126.3, 127.0, 130.5, 133.3, 138.3, 151.7, 157.7, 158.7, 156.0, 162.9, 165.6, 174.7; MS (ES⁺) *m/z* calcd. for C₂₅H₂₉N₉O₂S: 519.62; found: 520.2 (M+H⁺); HRMS (ESI) calcd. for C₂₅H₃₀N₉O₂S: 520.2243; found: 520.2239 (M+H⁺); HPLC (condition A) *t*_R = 21.89 min, 98.7%, (condition B) *t*_R = 23.25 min, 98.9%.

4.1.4.7.

N-[5-(tert-butyl)-3-isoxazolyl]-N'-[4-(2-[2-methyl-6-(4-methylpiperazino)-4-pyrimidinyl]amino)-1,3-thiazol-4-yl]phenyl]urea (7g)

Mp 330–331 °C. ¹H NMR (400 MHz, DMSO-*d*₆): δ 11.13 (s, 1H), 9.53 (s, 1H), 8.93 (s, 1H), 7.67 (s, 1H), 7.53–7.47 (m, 4H), 6.51 (s, 1H), 6.04 (s, 1H), 3.50 (br s, 4H), 2.41 (s, 3H),

2.36 (t, $J = 4.8$ Hz, 4H), 2.21 (s, 3H), 1.30 (s, 9H); ^{13}C NMR (100 MHz, DMSO- d_6) δ 26.1, 28.8, 32.9, 43.7, 46.2, 54.6, 82.6, 92.9, 119.4, 126.3, 126.9, 130.4, 133.3, 138.3, 151.7, 157.7, 158.6, 158.8, 162.8, 165.6, 180.7; MS (ES^+) m/z Calcd for $\text{C}_{27}\text{H}_{33}\text{N}_9\text{O}_2\text{S}$: 547.25; found: 548.3 ($\text{M}+\text{H}^+$); HRMS (ESI) calcd. for $\text{C}_{27}\text{H}_{34}\text{N}_9\text{O}_2\text{S}$: 548.2556; found: 548.2553 ($\text{M}+\text{H}^+$); HPLC (condition A) $t_R = 25.28$ min, 95.6%, (condition B) $t_R = 26.66$ min, 95.5%.

4.1.4.8.

N-(5-ethyl-3-isoxazolyl)-*N'*-[4-(2-[6-(4-ethylpiperazino)-2-methyl-4-pyrimidinyl]amino-1,3-thiazol-5-yl)phenyl]urea Dihydrochloride (**7h**)

Mp 259–260 °C. ^1H NMR (400 MHz, DMSO- d_6): δ 11.12 (s, 1H), 9.48 (s, 1H), 8.95 (s, 1H), 7.66 (s, 1H), 7.48 (ABq, $\Delta\nu_{\text{AB}} = 16.4$ Hz, $J_{\text{AB}} = 8.8$ Hz, 4H), 6.55 (s, 1H), 6.05 (s, 1H), 3.50 (br s, 4H), 2.70 (q, $J = 7.6$ Hz, 2H), 2.41–2.32 (m, 9H), 1.22 (t, $J = 7.6$ Hz, 3H), 1.03 (t, $J = 7.2$ Hz, 3H); ^{13}C NMR (75 MHz, DMSO- d_6) δ 11.9, 12.4, 20.2, 26.1, 44.0, 52.1, 52.4, 82.6, 94.7, 119.5, 126.3, 127.0, 130.4, 133.3, 138.3, 151.7, 157.7, 158.6, 159.0, 162.9, 165.6, 174.7; MS (ES^+) m/z calcd. for $\text{C}_{26}\text{H}_{31}\text{N}_9\text{O}_2\text{S}$: 533.23; found: 534.2 ($\text{M}+\text{H}^+$); HRMS (ESI) calcd. for $\text{C}_{26}\text{H}_{32}\text{N}_9\text{O}_2\text{S}$: 534.2400; found: 534.2390 ($\text{M}+\text{H}^+$); HPLC (condition A) $t_R = 22.75$ min, 100%, (condition B) $t_R = 24.41$ min, 98.9%.

4.1.4.9.

N-[4-(2-[6-(3-aminotetrahydro-1H-1-pyrrolyl)-2-methyl-4-pyrimidinyl]amino-1,3-thiazol-5-yl)phenyl]-*N'*-(5-ethyl-3-isoxazolyl)urea Dihydrochloride (**7i**)

Mp 267–268 °C. ^1H NMR (400 MHz, DMSO- d_6): δ 8.94 (s, 1H), 7.63 (s, 1H), 7.48 (ABq, Δv_{AB} = 14.0 Hz, J_{AB} = 8.4 Hz, 4H), 6.53 (s, 1H), 5.73 (s, 1H), 3.37 (br s, 7H, overlapping with water peak), 2.69 (q, J = 7.2 Hz, 2H), 2.37 (s, 3H), 1.99 (br s, 1H), 1.67 (br s, 1H), 1.19 (t, J = 7.6 Hz, 3H); ^{13}C NMR (100 MHz, DMSO- d_6) δ 11.9, 20.2, 26.0, 45.0, 50.8, 54.7, 60.2, 82.3, 94.7, 119.4, 126.2, 126.9, 130.3, 133.2, 138.4, 151.8, 156.7, 158.8, 159.0, 160.9, 165.4, 174.6; MS (ES^+) m/z calcd. for $\text{C}_{24}\text{H}_{27}\text{N}_9\text{O}_2\text{S}$: 505.20 ; found: 506.2 ($\text{M}+\text{H}^+$); HRMS (ESI) calcd. for $\text{C}_{24}\text{H}_{28}\text{N}_9\text{O}_2\text{S}$: 506.2087; found: 506.2083 ($\text{M}+\text{H}^+$); HPLC (condition A) t_R = 19.72 min, 99.7%, (condition B) t_R = 21.87 min, 98.3%.

4.1.4.10.

N-(5-cyclopropyl-3-isoxazolyl)-*N'*-[4-(2-[6-(4-ethylpiperazino)-2-methyl-4-pyrimidinyl]amino-1,3-thiazol-5-yl)phenyl]urea (**7j**)

Mp 271–272 °C. ^1H NMR (400 MHz, DMSO- d_6): δ 11.12 (s, 1H), 9.44 (s, 1H), 8.88 (s, 1H), 7.65 (s, 1H), 7.48 (ABq, Δv_{AB} = 18.4 Hz, J_{AB} = 8.8 Hz, 4H), 6.47 (s, 1H), 6.03 (s, 1H), 3.48 (br s, 4H), 2.40 (br s, 7H), 2.34 (q, J = 7.2 Hz, 2H), 2.12-2.06 (m, 1H), 1.05-0.99 (m, 5H), 0.89-0.85 (m, 2H); ^{13}C NMR (75 MHz, DMSO- d_6) δ 8.3, 8.5, 12.4, 26.1, 44.0, 52.0, 52.4, 82.6, 93.0, 119.5, 126.3, 126.6, 130.5, 131.9, 138.3, 151.6, 157.7, 158.7, 159.0, 162.9, 165.6, 174.6; MS (ES^+) m/z calcd. for $\text{C}_{27}\text{H}_{31}\text{N}_9\text{O}_2\text{S}$: 545.23; found: 546.2 ($\text{M}+\text{H}^+$); HRMS (ESI) calcd. for $\text{C}_{27}\text{H}_{32}\text{N}_9\text{O}_2\text{S}$: 546.2400; found: 546.2390 ($\text{M}+\text{H}^+$); HPLC (condition A) t_R = 22.79 min, 98.4%, (condition B) t_R = 24.65 min, 95.6%.

4.1.5.

N-[4-(2-{[6-(4-ethylpiperazin-1-yl)-2-methylpyrimidin-4-yl]amino}-1,3-thiazol-5-yl)phenyl]benzenesulfonamide (**8**)

To a solution of **6** (1.0 equiv) in pyridine at room temperature was added benzenesulfonyl chloride (1.1 equiv). After 2 h of stirring at room temperature, the reaction mixture was evaporated to dryness. The residue was suspended in saturated NaHCO₃ solution and the resulting suspension was vigorously stirred at room temperature for 1 h. The resultant solid was collected by filtration and recrystallized from EtOAc/CH₃OH to yield **8**. Mp 281–282 °C. ¹H NMR (300 MHz, DMSO-*d*₆): δ 11.13 (s, 1H), 10.35 (s, 1H), 7.79-7.76 (d, *J* = 8.1 Hz, 2H), 7.63-7.53 (m, 4H), 7.44 (d, *J* = 8.7 Hz, 2H), 7.11 (d, *J* = 8.7 Hz, 2H), 5.76 (s, 1H), 4.08 (br s, 1H), 3.33 (s, 1H), 3.16 (d, *J* = 5.4 Hz, 2H), 2.41-2.32 (m, 9H), 1.02 (t, *J* = 7.2 Hz, 3H); ¹³C NMR (75 MHz, DMSO-*d*₆) δ 12.4, 26.0, 44.0, 49.1, 52.1, 52.4, 82.6, 121.2, 126.5, 127.1, 128.6, 129.7, 129.9, 133.4, 133.9, 136.8, 140.0, 157.6, 159.0, 162.8, 165.6; MS (ES⁺) *m/z* calcd. for C₂₆H₂₉N₇O₂S₂: 535.68; found: 536.2 (M+H⁺); HRMS (ESI) calcd. for C₂₆H₃₀N₇O₂S₂: 536.1902; found: 536.1902 (M+H⁺); HPLC (condition A) *t*_R = 21.89 min, 99.4%, (condition B) *t*_R = 24.59 min, 98.8%.

4.1.6.

Benzyl

[4-(2-{[6-(4-ethylpiperazin-1-yl)-2-methylpyrimidin-4-yl]amino}-1,3-thiazol-5-yl)phenyl]carb

amate Dihydrochloride (**9**).

To a solution of **6** (1.0 equiv) in pyridine at room temperature was added benzyl chloroformate (1.1 equiv). After 4 h of stirring at room temperature, the reaction mixture was evaporated to dryness. The residue was suspended in saturated NaHCO₃ solution and the resulting suspension was vigorously stirred at room temperature for 1 h. The resultant solid was collected by filtration and recrystallized from CH₃CN/CH₃OH to yield **9**. Mp 260–261 °C. ¹H NMR (400 MHz, DMSO-*d*₆): δ 11.13 (s, 1H), 9.86 (s, 1H), 8.14 (s, 1H), 7.65 (s, 1H), 7.50–7.33 (m, 10H), 6.05 (s, 1H), 5.16 (s, 2H), 2.44–2.35 (m, 11H), 1.03 (t, *J* = 7.2 Hz, 3H); ¹³C NMR (100 MHz, DMSO-*d*₆) δ 12.4, 26.1, 44.0, 52.1, 52.4, 66.2, 82.6, 119.1, 126.3, 126.9, 128.5, 128.6, 128.9, 130.4, 133.3, 137.0, 138.4, 153.7, 157.7, 158.7, 162.8, 165.6; MS (ES⁺) *m/z* calcd. for C₂₈H₃₁N₇O₂S: 529.66; found: 530.3 (M+H⁺); HRMS (ESI) calcd. for C₂₈H₃₂N₇O₂S: 530.2338; found: 530.2335 (M+H⁺); HPLC (condition A) *t*_R = 26.33 min, 99.1%, (condition B) *t*_R = 28.07 min, 99.1%.

4.1.7.

N-[4-(2-{[6-(4-ethylpiperazin-1-yl)-2-methylpyrimidin-4-yl]amino}-1,3-thiazol-5-yl)phenyl]benzamide (**10**)

To a solution of **6** (1.0 equiv) in pyridine at room temperature was added benzoyl chloride (1.1 equiv). After 0.5 h of stirring at room temperature, the resultant solid was collected by filtration and washed with CH₃CN to yield **10**. Mp 324–325 °C. ¹H NMR (400

MHz, DMSO-*d*₆): δ 11.33 (s, 1H), 11.09 (s, 1H), 10.38 (s, 1H), 7.97 (d, *J* = 6.8 Hz, 1H), 7.85 (d, *J* = 8.0 Hz, 1H), 7.77 (s, 1H), 7.59-7.54 (m, 4H), 6.17 (s, 1H), 4.33 (br s, 1H), 3.53-3.23 (m, 8H), 3.14-2.99 (m, 4H), 2.46 (s, 1H), 1.36 (s, 3H); ¹³C NMR (100 MHz, DMSO-*d*₆) δ 9.2, 26.0, 40.6, 50.0, 51.0, 83.4, 121.3, 125.7, 126.0, 127.9, 128.2, 128.8, 130.7, 132.1, 133.6, 135.3, 138.6, 157.9, 158.6, 162.3, 165.9; MS (ES⁺) *m/z* calcd. for C₂₇H₂₉N₇O₅: 499.64; found: 500.2 (M+H⁺); HRMS (ESI) calcd. for C₂₇H₃₀N₇O₅S: 500.2233; found: 500.2225 (M+H⁺). HPLC (condition A) *t*_R = 22.83 min, 97.2%, (condition B) *t*_R = 24.77 min, 95.3%.

4.1.8.

*N*1-5-[4-[(5-methyl-3-isoxazolyl)amino]carbonylamino]phenyl]-1,3-thiazol-2-yl-4-(2-morpholinoethoxy)benzamide (**12**)

To a solution of **4** (1.0 equiv) in pyridine at room temperature was added 4-[2-(morpholin-4-yl)ethoxy]benzoyl chloride (1.1 equiv). After 2 h of stirring at room temperature, the reaction was worked up as described for compounds **6** to yield crude product **11** without further purification. To a solution of **11** (1.0 equiv) in pyridine at room temperature was added (5-methyl-isoxazol-3-yl)-carbamic acid 4-nitro-phenyl ester (1.5 equiv). After 2 h of stirring at room temperature, the reaction was worked up as described for compounds **6** and recrystallized from CH₃CN/CH₃OH to yield **12**. Mp 252–253 °C. ¹H NMR (400 MHz, DMSO-*d*₆): δ 10.75 (s, 1H), 10.20 (s, 1H), 9.80 (s, 1H), 7.96 (d, *J* = 8.8 Hz, 2H), 7.84-7.72 (m, 3H), 7.58 (d, *J* = 8.8 Hz, 2H), 7.08 (d, *J* = 8.8 Hz, 2H), 6.61 (s, 1H), 4.18 (t, *J* =

5.6 Hz, 2H), 3.58 (t, $J = 4.4$ Hz, 4H), 2.72 (t, $J = 5.6$ Hz, 2H), 2.47 (t, $J = 4.4$ Hz, 4H), 2.39 (s, 3H); ^{13}C NMR (100 MHz, DMSO- d_6) δ 12.6, 54.0, 57.4, 66.0, 66.6, 96.0, 114.6, 121.1, 126.2, 127.0, 127.2, 130.1, 130.9, 132.6, 139.2, 151.6, 154.2, 158.5, 161.6, 165.3, 170.2; MS (ES^+) m/z calcd. for $\text{C}_{27}\text{H}_{28}\text{N}_6\text{O}_5\text{S}$: 548.18; found: 549.2 ($\text{M}+\text{H}^+$); HRMS (ESI) calcd. for $\text{C}_{27}\text{H}_{29}\text{N}_6\text{O}_5\text{S}$: 549.1920; found: 549.1912 ($\text{M}+\text{H}^+$); HPLC (condition A) $t_R = 19.81$ min, 96.4%, (condition B) $t_R = 21.72$ min, 93.6%.

4.1.9. General procedure for the preparation of hydrochloride and formic acid salts

To a solution of compounds **7** (1.0 equiv) in methanol at room temperature was added 6 N HCl (4.0 equiv) or formic acid (2.0 equiv) and the resultant mixture was stirred for 0.5 h. The reaction mixture was evaporated to dryness and the residue suspended in EtOH. The suspension was sonicated for 1 h and the resultant solid was collected by filtration. The filtered solid was washed with EtOH and dried in vacuo to yield the corresponding salts.

4.2. Biology

4.2.1. Biochemical Kinase Assays

FLT3 – GST-FLT3-KD^{WT} containing the FLT3 kinase catalytic domain (residues Y567~S993) were expressed in Sf9 insect cells transfected the baculovirus containing pBac-PAK8-GST-FLT3-KD plasmid. The FLT3^{WT} Kinase-Glo assays were carried out in 96-well plates at 30 °C for 4 h and tested compound in a final volume of 50 μl including the following components: 75 ng GST-FLT3-KD^{WT} proteins, 25 mM HEPES, pH 7.4, 4 mM

MnCl₂, 10 mM MgCl₂, 2mM DTT, 0.02% Triton X-100, 0.1 mg/ml bovine serum albumin, 25 µM Her2 peptide substrate, 0.5 mM Na₃VO₄, and 1 µM ATP.

VEGFR2 – The recombinant GST-VEGFR2 (residues V789-V1356) containing kinase domain were expressed in Sf9 insect cells. The kinase assay were carried out in 96-well plates with tested compound in a final volume of 50 µl reaction at 30 °C for 120 minutes with following components: 25 mM HEPES pH 7.4, 10 mM MgCl₂, 4mM MnCl₂, 0.5mM Na₃VO₄, 2 mM DTT, 0.02% Triton X100, 0.01% BSA, 1 µM ATP, 2 µM polyGlu4:Tyr peptide, 50~100 ng recombinant VEGFR2.

Aurora A Kinase – The recombinant GST-Aurora A (residues S123-S401) containing kinase domain were expressed in Sf9 insect cells. The kinase assay were carried out in 96-well plates with tested compound in a final volume of 50 µl reaction at 37 °C for 90 minutes with following components : 50 mM Tris-HCl pH 7.4, 10 mM NaCl, 10 mM MgCl₂, 0.01% BSA, 5 µM ATP, 1mM DTT and 15 µM tetra(LRRASLG) peptide, and 150 ng recombinant Aurora A.

Following incubation, 50 µl Kinase-Glo Plus Reagent (Promega, Madison, WI, USA) was added and the mixture was incubated at 25 °C for 20 min. A 70-µl aliquot of each reaction mixture was transferred to a black microtiter plate and the luminescence was measured on Wallac Vector 1420 multilabel counter (PerkinElmer, Shelton, CT, USA).

4.2.2. Cell Lines and Reagents

The five leukemic cell lines 32D, RS4;11, MV4;11, U937 and K562 were purchased from American Type Culture Collection (ATCC, Manassas, VA, USA). MOLM-13 cells were obtained from the Deutsche Sammlung von Microorganismen und Zellkulturen GmbH (DSMZ, Braunschweig, Germany). Murine pro-B lymphocyte 32D cell lines stably

transfected with expression vectors that encoded human FLT3 containing an ITD mutation (32D-ITD cells), ITD and D835Y (32D-ITD/D835Y cells), ITD and D835V (32D-ITD/D835V cells), ITD and D835F (32D-ITD/D835F cells), and ITD and F691L (32D-ITD/F691L cells) mutations, which lead to constitutive activation of the FLT3 downstream signaling proteins, were generated by Dr. H. Eugene Liu, Division of Hematology and Oncology, Department of Internal Medicine, Wan Fang Hospital, Taipei Medical University, Taipei, Taiwan. All leukemic cell lines were grown in RPMI 1640 with 10% fetal bovine serum (FBS) (Fisher Scientific, Pittsburgh, PA, USA). The HEK293T and FLT3-transfected HEK293T cells were cultured in DMEM (Invitrogen, USA) medium with 10% FBS fetal bovine serum. The anti-FLT3 (sc-480, Santa Cruz Biotechnology, Santa Cruz, CA, USA), anti-pFLT3-Tyr591 (#3461, Cell Signaling Technology, Beverly, MA, USA) and anti- β -actin (Gtx110546, GeneTex, Irvine, CA, USA) antibodies were purchased for Western blotting analysis.

4.2.3. Cell Viability

The cell viability was assessed with an MTS assay as previously described.²⁹ 32D-ITD, 32D-ITD/D835Y, 32D-ITD/D835V, 32D-ITD/D835F and 32D-ITD/F691L cells were seeded in 96-well plates at 1×10^4 cells/mL (100 μ L per well) for 24 h incubation, and then test compound (at various concentrations in dimethyl sulfoxide [DMSO]) was added to the culture medium for 72 h incubation. The cell viability was determined by MTS assay (Promega,

Madison, WI, USA).

4.2.4. Western blot analysis

Protein lysates were prepared from cell line, resolved by SDS-PAGE, and transferred onto membrane according to our previous protocols.²⁹ After transfer to membrane, proteins were immunoblotted with appropriate antibodies and detected using the SuperSignal reagent (Pierce, Rockford, IL, USA) followed by exposure to X-ray film.

4.3. Pharmacokinetics

Male Sprague–Dawley rats weighing 300–400 g each (8–12 weeks old) were obtained from BioLASCO (Taiwan Co., Ltd, Ilan, Taiwan). The animal studies were performed according to NHRI institutional animal care and committee-approved procedures. Animals were surgically prepared with a jugular-vein cannula one day before dosing and fasted overnight (for approximately 18–20 h) before dosing. Water was available *ad libitum* throughout the experiment. Food was provided at 4 h after dosing. A single 2.0 mg/kg and 10 mg/kg dose of compound, as a PEG400/DMA (80/20, v/v) solution, was separately administered to groups of 3 rats each intravenously (IV) and oral gavage (PO), respectively. Each animal received 2 or 10 ml of the dosing solution per kg of body weight for IV and PO, respectively. At 0 (before dosing), 2, 5 (IV only), 15, and 30 min and at 1, 2, 4, 6, 8, and 24 h after dosing, a blood sample (0.15 ml) was collected from each animal through the jugular-vein cannula and stored in ice (0–4 °C). Immediately after collecting the blood sample, 150 µl of physiological saline (containing 30 Units of heparin per ml) was injected into the rat through the jugular-vein cannula. Plasma was separated from the blood by centrifugation (14 000 g for 15 min at 4 °C in a Beckman Model Allegra™ 6R centrifuge) and stored in a freezer (-20 °C). All samples were analysed for the parent drug by LC-MS/MS. Data were

acquired through selected reaction ion monitoring. Plasma concentration data were analyzed with non-compartmental method.

Male ICR mice weighing 25–35 g each were obtained from BioLASCO (Taiwan Co., Ltd, Ilan, Taiwan). The animal studies were performed according to NHRI institutional animal care and committee-approved procedures. Single 2.0 mg/kg intravenous dose of compound was administered to a total of 33 male mice and single 10 mg/kg oral dose was administered to a total of 27 male mice. Each mouse was given 100 μ L of the IV dosing solution intravenously by tail-vein injection and 200 μ L of the PO dosing solution orally by gavage. Animals that received the IV dose were not fasted and that received the PO dose were fasted overnight prior to dosing. At 0 (immediately before dosing), 2 (IV only), 5 (IV only), 15 and 30 min and at 1, 2, 4, 6, 8, 16 and 24 hr after dosing, blood (~500 μ L) was collected from groups of 3 mice at each time point by cardio puncture and stored in ice (0–4 °C). EDTA was used as the anticoagulant. Plasma was separated from the blood by centrifugation (3000 rpm for 15 min at 4 °C in a Beckman Model Allegra 6R centrifuge) and stored in a freezer (-20 °C). Control plasma was obtained from mice receiving no compound for use of constructing the standard curve and for the preparation of quality control (QC) samples. All samples were analyzed for the parent compound by LC-MS/MS.

4.4. Efficacy in xenograft and myeloproliferative mouse models

Human leukemia cells (MOLM-13 and MV4;11 cell lines) and 32D cells (a murine

IL-3-dependent myeloid cell line, 32D/FLT3-ITD-D835Y) were cultured and maintained in flasks with RPMI-1640 medium (Gibco, Life technologies™, Corporation). The culture medium was supplemented with 10% fetal bovine serum (FBS). The cells were incubated at 37 °C in a humidified atmosphere containing 5% CO₂.

The animal use protocol was approved by The Institutional Care and Use Committee of the Wan Fang Hospital, Taipei, Taiwan and National Health Research Institutes (Protocol No: NHRI-IACUC-103024). Briefly, Nude mice (*Nu-FoxI^{nu}*) and SCID mice (CB17/Icr-Prkdc^{scid}/IcrIcoCrIBltw) of six weeks old were purchased from BioLasco, Taiwan Co., Ltd. (Ilan, Taiwan). Animals were fed standard mice chow with water available *ad libitum*. The animals were housed in group cages under a 12 hour light/dark cycle. Cells were suspended in a volume that 100 µl contains 5x10⁶ 32D/FLT3-ITD-D835Y or MV4;11 cells per SC inoculation in nude mice. MOLM-13 cell suspended in 100 µl PBS contains 5x10⁶ via SCID mice tail vein injection for survival rate study. The animals will be grouped and treated with compound **7h** or controls. Animals were treated with compound **3** at 10 mg/kg, **7 h** (10 and 25 mg/kg (PO) or vehicle by gavage for five consecutive days a week for two continuous weeks for MV4;11 subcutaneously xenograft and days 2-5 and 8-12 for MOLM-13 survival rate study. In drug-resistant xenograft tumor model, the 32D/FLT3-ITD-D835Y bearing animals will be grouped and treated with compound **3** and compound **7 h** at 10 mg/kg or vehicle by gavage for five consecutive days a week for four continuous weeks.

Tumor size was measured with a digital caliper, and the tumor volume in mm³ was

calculated by the formula: $\text{Volume} = (\text{length} \times \text{width}^2)/2$. Tumor-bearing mice were randomized when the size of a growing tumor $\sim 150 \text{ mm}^3$. All mice were monitored daily for signs of toxicity. Body weight and tumor size were measured twice a week. Daily observations of health changes are possible during experimental time. At the end of the studies, animals will then be euthanized by carbon dioxide inhalation followed by cervical dislocation.

Acknowledgments

The National Health Research Institutes and National Science Council of Taiwan (NSC 103-2325-B-400 -013 -) financially supported the study.

Appendix A. Supplementary data

Supplementary data related to this article can be found at

References

- [1] Tallman, M. S.; Gilliland, D. G.; Rowe, J. M. Drug therapy for acute myeloid leukemia. *Blood* **2005**, *106*, 1154-1163.
- [2] Shankar, D. B.; Li, J.; Tapang, P.; Owen McCall, J.; Pease, L. J.; Dai, Y.; Wei, R. Q.; Albert, D. H.; Bouska, J. J.; Osterling, D. J.; Guo, J.; Marcotte, P. A.; Johnson, E. F.; Soni, N.; Hartandi, K.; Michaelides, M. R.; Davidsen, S. K.; Priceman, S. J.; Chang, J.

- C.; Rhodes, K.; Shah, N.; Moore, T. B.; Sakamoto, K. M.; Glaser, K. B. ABT-869, a multitargeted receptor tyrosine kinase inhibitor: inhibition of FLT3 phosphorylation and signaling in acute myeloid leukemia. *Blood* **2007**, *109*, 3400-3408.
- [3] Gilliland, D. G.; Griffin, J. D. The roles of FLT3 in hematopoiesis and leukemia. *Blood* **2002**, *100*, 1532-1542.
- [4] Stirewalt, D. L.; Radich, J. P. The role of FLT3 in haematopoietic malignancies. *Nat. Rev. Cancer* **2003**, *3*, 650-665.
- [5] Kottaridis, P. D.; Gale, R. E.; Frew, M. E.; Harrison, G.; Langabeer, S. E.; Belton, A. A.; Walker, H.; Wheatley, K.; Bowen, D. T.; Burnett, A. K.; Goldstone, A. H.; Linch, D. C. The presence of a FLT3 internal tandem duplication in patients with acute myeloid leukemia (AML) adds important prognostic information to cytogenetic risk group and response to the first cycle of chemotherapy: analysis of 854 patients from the United Kingdom Medical Research Council AML 10 and 12 trials. *Blood* **2001**, *98*, 1752-1759.
- [6] Fröhling, S.; Schlenk, R. F.; Breitruck, J.; Benner, A.; Kreitmeier, S.; Tobis, K.; Döhner, H.; Döhner, K. Prognostic significance of activating FLT3 mutations in younger adults (16 to 60 years) with acute myeloid leukemia and normal cytogenetics: a study of the AML Study Group Ulm. *Blood* **2002**, *100*, 4372-4380.
- [7] Kikushige, Y.; Yoshimoto, G.; Miyamoto, T.; Iino, T.; Mori, Y.; Iwasaki, H.; Niino, H.; Takenaka, K.; Nagafuji, K.; Harada, M.; Ishikawa, F.; Akashi, K. Human Flt3 is expressed at the hematopoietic stem cell and the granulocyte/macrophage progenitor

stages to maintain cell survival. *J. Immunol.* **2008**, *180*, 7358-7367.

- [8] Mizuki, M.; Fenski, R.; Halfter, H.; Matsumura, I.; Schmidt, R.; Müller, C.; Grüning, W.; Kratz-Albers, K.; Serve, S.; Steur, C.; Büchner, T.; Kienast, J.; Kanakura, Y.; Berdel, W. E.; Serve, H. Flt3 mutations from patients with acute myeloid leukemia induce transformation of 32D cells mediated by the Ras and STAT5 pathways. *Blood* **2000**, *96*, 3907-3914.
- [9] Abu-Duhier, F. M.; Goodeve, A. C.; Wilson, G. A.; Care, R. S.; Peake, I. R.; Reilly, J. T. Identification of novel FLT-3 Asp835 mutations in adult acute myeloid leukaemia. *Br. J. Haematol.* **2001**, *113*, 983-988.
- [10] Ozeki, K.; Kiyoi, H.; Hirose, Y.; Iwai, M.; Ninomiya, M.; Kodaera, Y.; Miyawaki, S.; Kuriyama, K.; Shimazaki, C.; Akiyama, H.; Nishimura, M.; Motoji, T.; Shinagawa, K.; Takeshita, A.; Ueda, R.; Ohno, R.; Emi, N.; Naoe, T. Biologic and clinical significance of the FLT3 transcript level in acute myeloid leukemia. *Blood* **2004**, *103*, 1901-1908.
- [11] Shiotsu, Y.; Kiyoi, H.; Ishikawa, Y.; Tanizaki, R.; Shimizu, M.; Umehara, H.; Ishii, K.; Mori, Y.; Ozeki, K.; Minami, Y.; Abe, A.; Maeda, H.; Akiyama, T.; Kanda, Y.; Sato, Y.; Akinaga, S.; Naoe, T. KW-2449, a novel multikinase inhibitor, suppresses the growth of leukemia cells with FLT3 mutations or T315I-mutated BCR/ABL translocation. *Blood* **2009**, *114*, 1607-1617.
- [12] Fischer, T.; Stone, R. M.; Deangelo, D. J.; Galinsky, I.; Estey, E.; Lanza, C.; Fox, E.; Ehninger, G.; Feldman, E. J.; Schiller, G. J.; Klimek, V. M.; Nimer, S. D.; Gilliland, D. G.;

- Dutreix, C.; Huntsman-Labed, A.; Virkus, J.; Giles, F. J. Phase IIB trial of oral Midostaurin (PKC412), the FMS-like tyrosine kinase 3 receptor (FLT3) and multi-targeted kinase inhibitor, in patients with acute myeloid leukemia and high-risk myelodysplastic syndrome with either wild-type or mutated FLT3. *J. Clin. Oncol.* **2010**, *28*, 4339-4345.
- [13] Auclair, D.; Miller, D.; Yatsula, V.; Pickett, W.; Carter, C.; Chang, Y.; Zhang, X.; Wilkie, D.; Burd, A.; Shi, H.; Rocks, S.; Gedrich, R.; Abriola, L.; Vasavada, H.; Lynch, M.; Dumas, J.; Trail, P. A.; Wilhelm, S. M. Antitumor activity of sorafenib in FLT3-driven leukemic cells. *Leukemia* **2007**, *21*, 439-445.
- [14] Chao, Q.; Sprankle, K. G.; Grotzfeld, R. M.; Lai, A. G.; Carter, T. A.; Velasco, A. M.; Gunawardane, R. N.; Cramer, M. D.; Gardner, M. F.; James, J.; Zarrinkar, P. P.; Patel, H. K.; Bhagwat, S. S. Identification of N-(5-tert-butyl-isoxazol-3-yl)-N'-{4-[7-(2-morpholin-4-yl-ethoxy)imidazo[2,1-b][1,3]benzothiazol-2-yl]phenyl}urea dihydrochloride (AC220), a uniquely potent, selective, and efficacious FMS-like tyrosine kinase-3 (FLT3) inhibitor. *J. Med. Chem.* **2009**, *52*, 7808-7816.
- [15] Ustun, C.; DeRemer, D. L.; Jillella, A. P.; Bhalla, K. N. Investigational drugs targeting FLT3 for leukemia. *Expert Opin. Investig. Drugs* **2009**, *18*, 1445-1456.
- [16] Knapper, S. The clinical development of FLT3 inhibitors in acute myeloid leukemia. *Expert Opin. Investig. Drugs* **2011**, *20*, 1377-1395.

- [17] Pratz, K.W.; Sato, T.; Murphy, K. M.; Stine, A.; Rajkhowa, T.; Levis, M. FLT3-mutant allelic burden and clinical status are predictive of response to FLT3 inhibitors in AML. *Blood* **2010**, *115*, 1425-1432.
- [18] Smith, C. C.; Wang, Q.; Chin, C. S.; Salerno, S.; Damon, L. E.; Levis, M. J.; Perl, A. E.; Travers, K. J.; Wang, S.; Hunt, J. P.; Zarrinkar P. P.; Schadt, E. E.; Kasarskis, A.; Kuriyan, J.; Shah, N. P. Validation of ITD mutations in FLT3 as a therapeutic target in human acute myeloid leukaemia. *Nature* **2012** *485*, 260-263.
- [19] Levis, M. FLT3 mutations in acute myeloid leukemia: what is the best approach in 2013? *Hematology Am. Soc. Hematol. Educ. Program* **2013**, *2013*, 220-226.
- [20] Heidel, F. 1.; Solem, F. K.; Breitenbuecher, F.; Lipka, D. B.; Kasper, S.; Thiede, M. H.; Brandts, C.; Serve, H.; Roesel, J.; Giles, F.; Feldman, E.; Ehninger, G.; Schiller, G. J.; Nimer, S.; Stone, R. M.; Wang, Y.; Kindler, T.; Cohen, P. S.; Huber, C.; Fischer, T. Clinical resistance to the kinase inhibitor PKC412 in acute myeloid leukemia by mutation of Asn-676 in the FLT3 tyrosine kinase domain. *Blood* **2006**, *107*, 293–300.
- [21] Man, C. H.; Fung, T. K.; Ho, C.; Han, H. H.; Chow, H. C.; Ma, A. C.; Choi, W. W.; Lok, S.; Cheung, A. M.; Eaves, C.; Kwong, Y. L.; Leung, A. Y. Sorafenib treatment of FLT3-ITD(+) acute myeloid leukemia: favorable initial outcome and mechanisms of subsequent nonresponsiveness associated with the emergence of a D835 mutation. *Blood* **2012**, *119*, 5133–5143.
- [22] Kesarwani, M.; Huber, E.; Azam, M. Overcoming AC220 resistance of FLT3-ITD by

SAR302503. *Blood Cancer J.* **2013**, *3*, e138.

- [23] Smith, C. C.; Lasater, E. A.; Zhu, X.; Lin, K. C.; Stewart W. K.; Damon, L. E.; Salerno, S.; Shah, N. P. Activity of ponatinib against clinically-relevant AC220-resistant kinase domain mutants of FLT3-ITD. *Blood* **2013**, *121*, 3165-3171.
- [24] Lin, W. H.; Jiaang, W. T.; Chen, C. W.; Yen, K. J.; Hsieh, S. Y.; Yen, S. C.; Chen, C. P.; Chang, K. Y.; Chang, C. Y.; Chang, T. Y.; Huang, Y. L.; Yeh, T. K.; Chao, Y. S.; Chen, C. T.; Hsu, J. T. BPR1J-097, a novel FLT3 kinase inhibitor, exerts potent inhibitory activity against AML. *Br. J. Cancer*. **2012**, *106*, 475-481.
- [25] Lin, W. H.; Hsieh, S. Y.; Yen, S. C.; Chen, C. T.; Yeh, T. K.; Hsu, T.; Lu, C. T.; Chen, C. P.; Chen, C. W.; Chou, L. H.; Huang, Y. L.; Cheng, A. H.; Chang, Y. I.; Tseng, Y. J.; Yen, K. R.; Chao, Y. S.; Hsu, J. T.; Jiaang, W. T. Discovery and evaluation of 3-phenyl-1H-5-pyrazolylamine-based derivatives as potent, selective and efficacious inhibitors of FMS-like tyrosine kinase-3 (FLT3). *Bioorg. Med. Chem.* **2011**, *19*, 4173-4182.
- [26] Hsu, J. T.; Yeh, T. K.; Yen, S. C.; Chen, C. T.; Hsieh, S. Y.; Hsu, T.; Lu, C. T.; Chen, C. H.; Chou, L. H.; Chiu, C. H.; Chang, Y. I.; Tseng, Y. J.; Yen, K. R.; Chao, Y. S.; Lin, W. H.; Jiaang, W. T. 3-Phenyl-1H-5-pyrazolylamine-based derivatives as potent and efficacious inhibitors of FMS-like tyrosine kinase-3 (FLT3). *Bioorg. Med. Chem. Lett.* **2012**, *22*, 4654-4659.
- [27] Lin, W. H.; Hsu, J. T.; Hsieh, S. Y.; Chen, C. T.; Song, J. S.; Yen, S. C.; Hsu, T.; Lu, C. T.;

- Chen, C. H.; Chou, L. H.; Yang, Y. N.; Chiu, C. H.; Chen, C. P.; Tseng, Y. J.; Yen, K. J.; Yeh, C. F.; Chao, Y. S.; Yeh, T. K.; Jiaang, W. T. Discovery of 3-phenyl-1H-5-pyrazolylamine derivatives containing a urea pharmacophore as potent and efficacious inhibitors of FMS-like tyrosine kinase-3 (FLT3). *Bioorg Med Chem.* **2013**, *21*, 2856-2867.
- [28] Lin, W. H.; Yeh, T. K.; Jiaang, W. T.; Yen, K. J.; Chen, C. H.; Huang, C. T.; Yen, S. C.; Hsieh, S. Y.; Chou, L. H.; Chen, C. P.; Chiu, C. H.; Kao, L. C.; Chao, Y. S.; Chen, C. T.; Hsu, J. T. Evaluation of the antitumor effects of BPR1J-340, a potent and selective FLT3 inhibitor, alone or in combination with an HDAC inhibitor, vorinostat, in AML cancer. *PLoS One* **2014**, *9*, e83160.
- [29] Yu, C.; Kancha, R. K.; Duyster, J. Targeting oncoprotein stability overcomes drug resistance caused by FLT3 kinase domain mutations. *PLoS One* **2014**, *9*, e97116.
- [30] Lee, B. W.; Lee, S. D. [5,5] Sigmatropic shift of *N*-phenyl-*N'*-(2-thiazolyl)hydrazines and *N,N'*-bis(2-thiazolyl)hydrazines into 2-amino-5-(*p*-aminophenyl)thiazoles and 5,5'-bis(2-aminothiazole) derivatives. *Tetrahedron Lett.* **2000**, *41*, 3883-3886.
- [31] Grese, T. A.; Cho, S.; Finley, D.; Godfrey, A. G.; Jones, C. D.; Lugar, C. W.; Martin, M. J.; Matsumoto, K.; Pennington, L. D.; Winter, M. W.; Adrian, M. D.; Cole, H. W.; Magee, D. E.; Phillips, D. L.; Rowley, E. R.; Short, L. L.; Glasebrook, A. L.; Bryant, H. U. Structure-Activity Relationships of Selective Estrogen Receptor Modulators: Modifications to the 2-Arylbenzothiophene Core of Raloxifene. *J. Med. Chem.* **1997**, *40*,

146-167.

- [32] Yao, Q.; Nishiuchi, R.; Li, Q.; Kumar, A. R.; Hudson, W. A.; Kersey, J. H. FLT3 expressing leukemias are selectively sensitive to inhibitors of the molecular chaperone heat shock protein 90 through destabilization of signal transduction-associated kinases. *Clin. Cancer Res.* **2003**, *9*, 4483-4493.
- [33] Yee, K. W.; O'Farrell, A. M.; Smolich, B. D.; Cherrington, J. M.; McMahon, G.; Wait, C. L.; McGreevey, L. S.; Griffith, D. J.; Heinrich, M. C. SU5416 and SU5614 inhibit kinase activity of wild-type and mutant FLT3 receptor tyrosine kinase. *Blood* **2002**, *100*, 2941-2949.
- [34] Fletcher, G. C.; Brokx, R. D.; Denny, T. A.; Hembrough, T. A.; Plum, S. M.; Fogler, W. E.; Sidor, C. F.; Bray, M. R. Author information ENMD-2076 is an orally active kinase inhibitor with antiangiogenic and antiproliferative mechanisms of action. *Mol. Cancer Ther.* **2011**, *10*, 126-137.

List of figure, scheme and table captions:

Figure 1. Structures of FLT3 inhibitors in the clinic.

Figure 2. Identification of 5-phenyl-thiazol-2-ylamine derivatives as FLT3 inhibitors.

Figure 3. HEK293T cells engineered to express FLT3-WT, FLT3-ITD, FLT3-ITD/D835Y or FLT3-ITD/F691L were analyzed. The HEK293T-FLT3 cells were treated with compound **7h** at various concentrations for 1 hr, and the FLT3 ligand (50 ng/mL) was added for 5 min to prepare the cell lysate for detection of changes in FLT3 phosphorylation by western blot analysis.

Figure 4. Comparison of antitumor efficacy of compounds **3** and **7h** in xenograft mouse models. (A) Human MV4;11 cells were implanted SC in nude mice. After the average size of the tumors reached to 200 mm³, mice were dosed with **3** or **7h** (qd, days 1-5 and 8-12) by oral gavage. The tumor size is expressed as the mean \pm SEM (n = 6-7/group). (B) MOLM-13 cells were IV inoculated into SCID mice. From the 2nd day after inoculation, mice were administered **7h** at 10 or 20 mg/kg or **3** at 10 mg/kg or vehicle (qd, days 2-5 and 8-12) by oral gavage (n = 6/group). (C) Mice were implanted subcutaneously (SC) with 32D/FLT3-ITD-D835Y cells. When the average tumor volume reached 200 mm³ in size, **3** or **7h** was administered orally at a dose of 10 mg/kg with a 5 days on/2 days off schedule for 4 weeks. The tumor size is expressed as the mean \pm SEM (n = 9/group).

Scheme 1. Reagents and conditions: (a) NaH, THF, 0 °C; (b) 2° amines, pyridine, 80 °C; (c) pyridine, phenyl isocyanate or (5-alkyl-isoxazol-3-yl)-carbamic acid 4-nitro-phenyl ester for **7** or **12**, benzenesulfonyl chloride for **8**, benzyl chloroformate for **9**, benzoyl chloride for **10**, rt; (d) CF₃COOH, rt for **7b**, **7d** and **7i**; (e) pyridine, benzoyl chloride with a morphine group, rt.

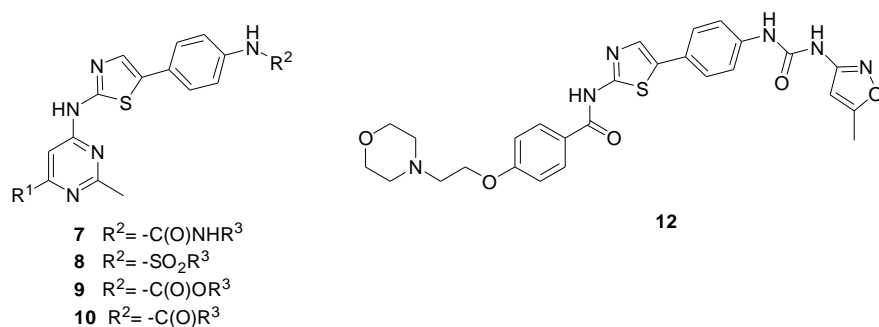
Table 1. Inhibition of enzymes and cell proliferation with thiazole analogues.

Table 2. Kinase inhibition profile of compounds **7h**.

Table 3. Inhibition of leukemia cell growth by **7h** and **1-3**.

Table 4. Activity of **3** and **7h** against 32D cells expressing native and drug-resistant mutants of FLT3-ITD.

Table 5. Pharmacokinetic profile of compound **7h**.

Table 1. Inhibition of enzymes and cell proliferation with thiazole analogues.

Compd	R^1	R^3	IC_{50} (μM) [*]			GI_{50} (μM)	Rats, PO 10 mg/kg $AUC_{(0-inf)}$ ng/mL *hr
			wt-FLT3	VEGFR2	Aurora A	MOLM-13	
7a		$-C_6H_5$	0.079	0.16	>10	0.024	undetectable
7b		$-C_6H_5$	0.073	0.053	0.15	0.016	undetectable
7c		4-Cl- C_6H_5 -	0.32	0.043	0.095	0.009	undetectable
7d		3-Cl- C_6H_5 -	0.020	0.031	0.27	0.024	undetectable
7e			0.010	0.015	0.056	0.001	313
7f			0.049	0.01	0.041	0.003	632
7g			0.022	0.055	0.038	0.014	—
7h			0.038	0.025	0.032	0.002	1075
7i			0.014	0.007	0.038	0.003	undetectable
7j			0.033	0.015	0.036	0.002	—
8		$-C_6H_5$	0.52	0.17	0.043	0.14	—
9		$-CH_2C_6H_5$	0.083	0.12	0.32	0.003	66
10		$-C_6H_5$	0.85	>1.0	0.14	0.019	—
12			0.58	0.37	0.025	0.21	—
1			0.037	0.25	0.080	0.055	—
2			0.044	0.042	3.8	0.056	—
3			0.069	0.43	>10	0.004	—

^{*} IC_{50} and GI_{50} values are the means of at least two independent experiments.

Table 2. Kinase inhibition profile of compounds **7h**.

Kinase	0.1 μ M % inhibition	Kinase	0.1 μ M % inhibition
FLT3	98	VEGFR2	85
PDGFR α	98	AURKB	85
SRC	97	TRKA	82
LYN A	96	VEGFR3	80
AURKA	96	BLK	78
RET	95	YES1	72
CSF1R	94	ABL1	66
LCK	92	RET V804L	65
PDGFR β	91	KIT	64
RET V804L	89	PDGFR α V561D	63
FGR	89	MEK1	62
LYN B	88	IRAK4	61
FLT3 D835Y	87	Tie2	61
RET Y791F	86	ABL1 T315I	51

Table 3. Inhibition of leukemia cell growth by **7h** and **1-3**.

Cell line*	Characterization	GI ₅₀ (μM)			
		7h	1	2	3
MOLM-13	AML-FLT3-ITD (heterozygous)	0.002	0.055	0.056	0.004
MV4;11	AML-FLT3-ITD (homozygous)	0.001	0.038	0.043	0.003
U937	AML-FLT3-negative	1.1	1.4	3.4	>20
RS4;11	ALL-wt-FLT3 (homozygous)	0.11	0.40	9.3	2.2
K562	CML-Bcr-Abl FLT3-negative	0.19	>20	7.3	>20

*AML, acute myelocytic leukemia; ALL, acute lymphoblastic leukemia; CML, chronic myelogenous leukemia

Table 4. Activity of **3** and **7h** against 32D cells expressing native and drug-resistant mutants of FLT3-ITD.

Cell line	GI ₅₀ (μM)*	
	7h	3
ITD alone	0.00001	0.00001
ITD-D835Y	0.006	0.016
ITD-D835V	0.004	0.027
ITD-D835F	0.038	0.15
ITD-F691L	0.070	0.22

*GI₅₀ values are the means of three independent experiments.

Table 5. Pharmacokinetic profile of compound **7h**.

Species	IV (dose: 2 mg/kg)		PO (dose: 10 mg/kg)			
	CL (mL/min/kg)	V _{ss} (L/kg)	T _{1/2} (hr)	C _{max} (ng/mL)	AUC _(0-inf) (ng/mL*hr)	F (%)
Rats	31.6	8.2	4.3	122	1,075	20
Mice	82	21	1.8	168	942	35

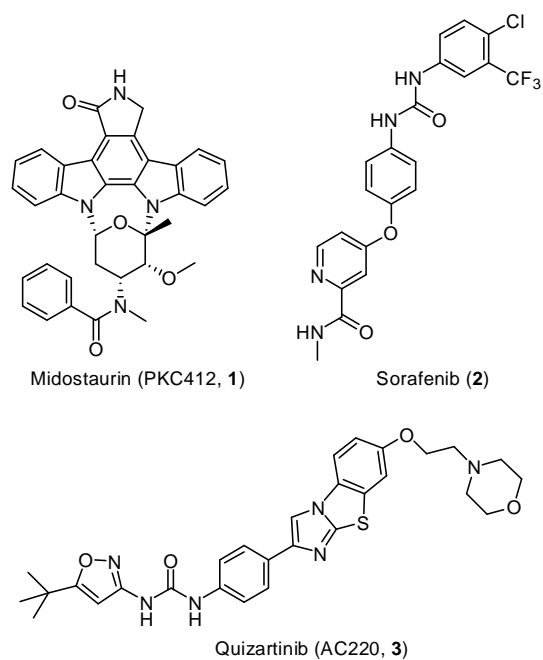


Figure 1. Structures of FLT3 inhibitors in the clinic.

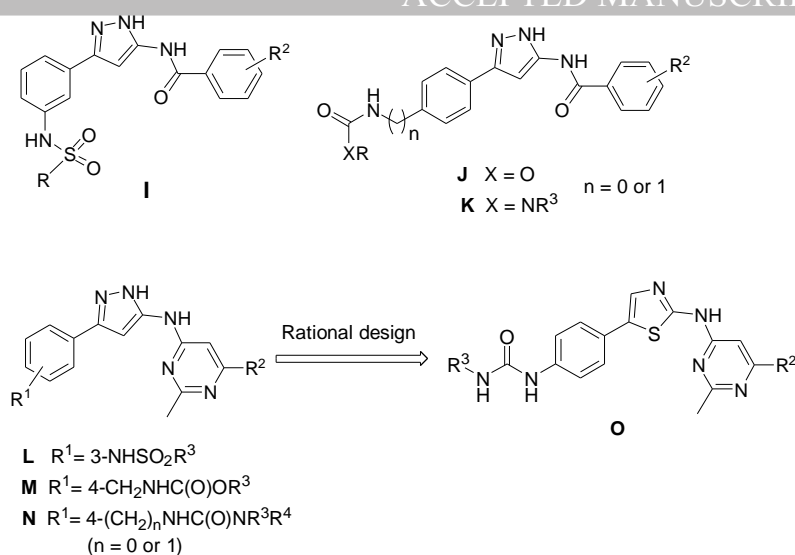


Figure 2. Identification of 5-phenyl-thiazol-2-ylamine derivatives as FLT3 inhibitors.

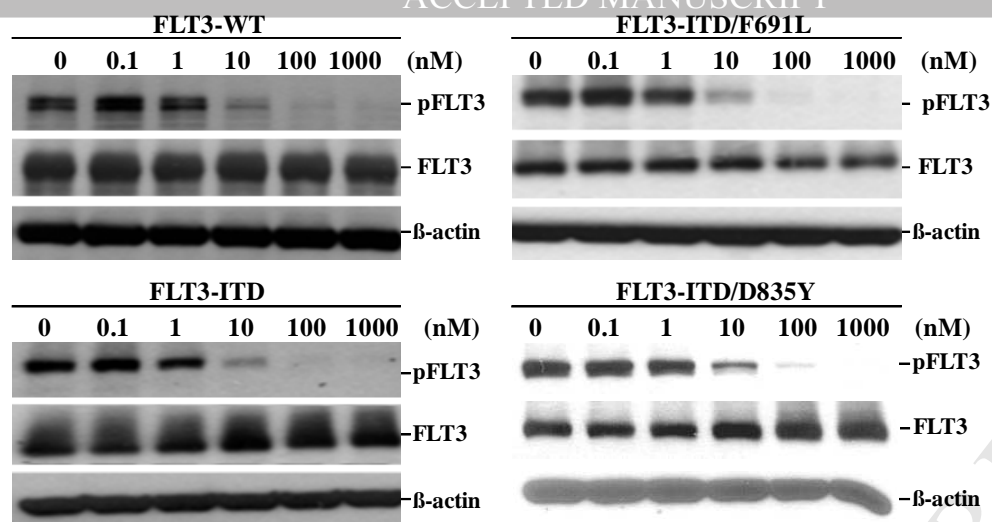


Figure 3. HEK293T cells engineered to express FLT3-WT, FLT3-ITD, FLT3-ITD/D835Y or FLT3-ITD/F691L were analyzed. The HEK293T-FLT3 cells were treated with compound **7h** at various concentrations for 1 hr, and the FLT3 ligand (50 ng/mL) was added for 5 min to prepare the cell lysate for detection of changes in FLT3 phosphorylation by western blot analysis.

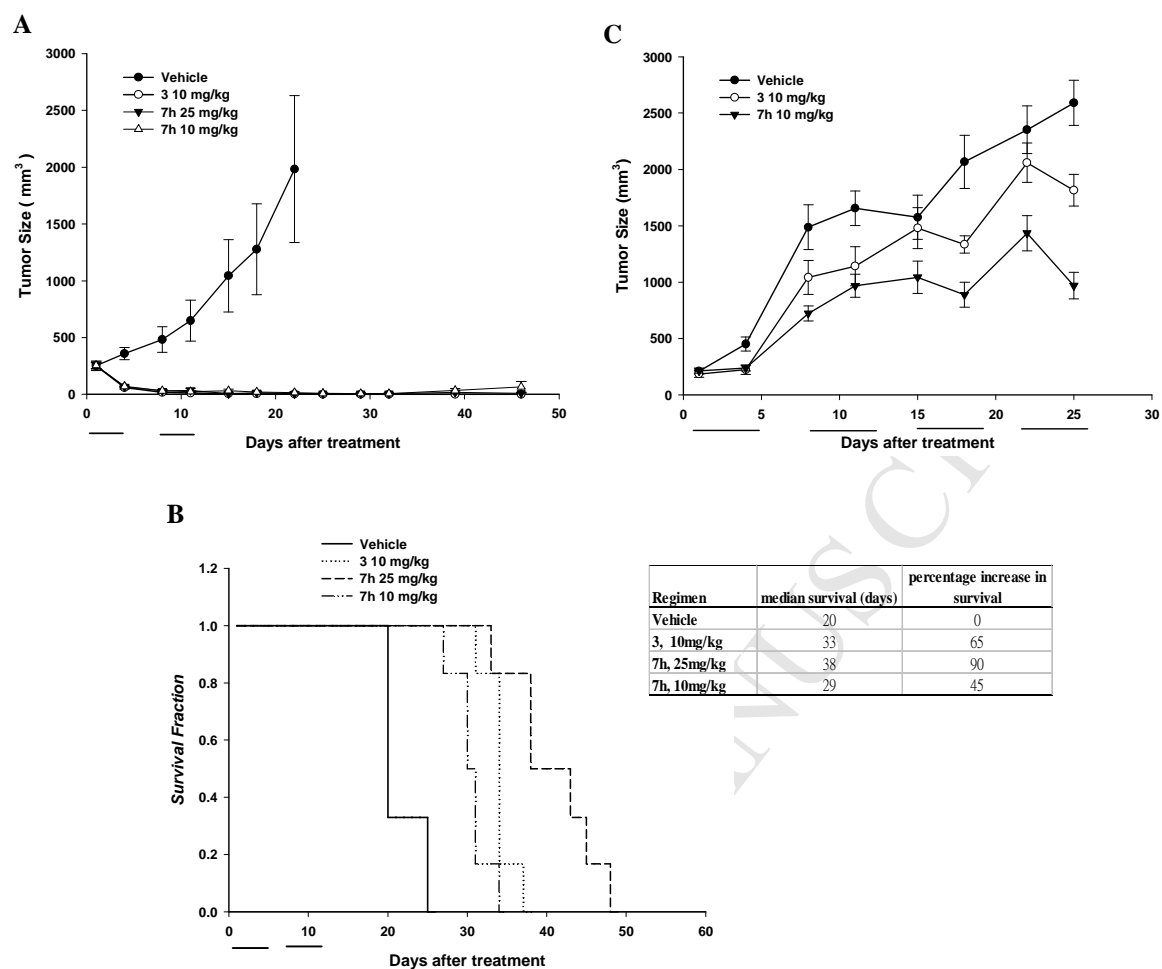
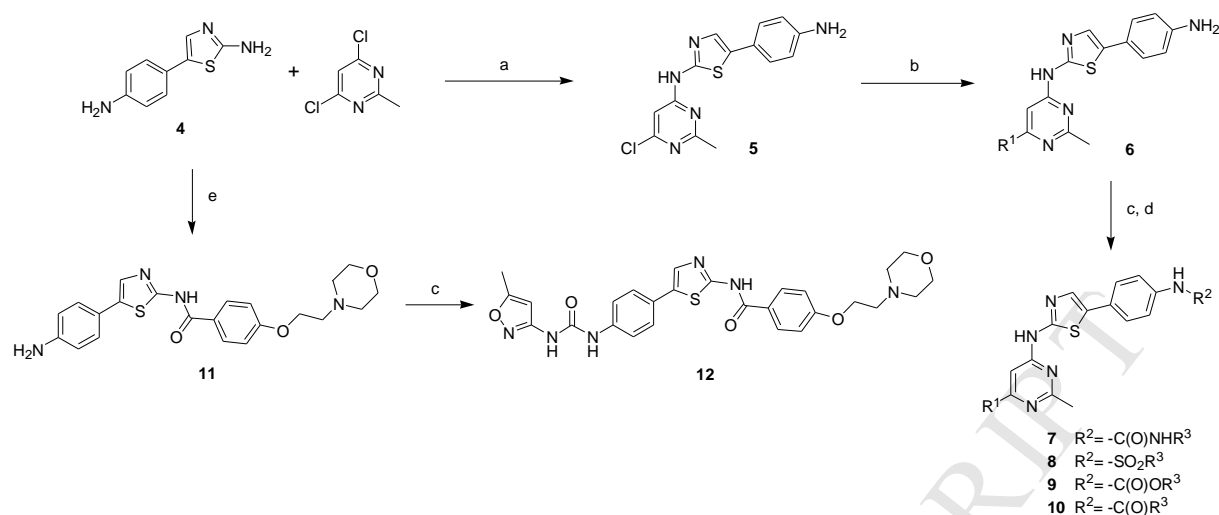


Figure 4. Comparison of antitumor efficacy of compounds **3** and **7h** in xenograft mouse models. (A) Human MV4;11 cells were implanted SC in nude mice. After the average size of the tumors reached to 200 mm³, mice were dosed with **3** or **7h** (qd, days 1-5 and 8-12) by oral gavage. The tumor size is expressed as the mean \pm SEM (n = 6-7/group). (B) MOLM-13 cells were IV inoculated into SCID mice. From the 2nd day after inoculation, mice were administered **7h** at 10 or 20 mg/kg or **3** at 10 mg/kg or vehicle (qd, days 2-5 and 8-12) by oral gavage (n = 6/group). (C) Mice were implanted subcutaneously (SC) with 32D/FLT3-ITD-D835Y cells. When the average tumor volume reached 200 mm³ in size, **3** or **7h** was administered orally at a dose of 10 mg/kg with a 5 days on/2 days off schedule for 4 weeks. The tumor size is expressed as the mean \pm SEM (n = 9/group).



Scheme 1. Reagents and conditions: (a) NaH, THF, 0 °C; (b) 2° amines, pyridine, 80 °C; (c) pyridine, phenyl isocyanate or (5-alkyl-isoxazol-3-yl)-carbamic acid 4-nitro-phenyl ester for **7** or **12**, benzenesulfonyl chloride for **8**, benzyl chloroformate for **9**, benzoyl chloride for **10**, rt; (d) CF₃COOH, rt for **7b**, **7d** and **7i**; (e) pyridine, benzoyl chloride with a morphine group, rt.

Highlights

1. Compound **7h** displayed potent antileukemic activity.
2. Oral administration of **7h** yielded complete tumor regression in MV4;11 xenografts.
3. Compound **7h** can overcome AC220-resistant kinase domain mutants of FLT3-ITD.

Supplementary material for

Identification of a potent 5-phenyl-thiazol-2-ylamine-based inhibitor of FLT3 with activity against drug resistance-conferring point mutations

Chiung-Tong Chen,^{1,#} John T.-A. Hsu,^{1,#} Wen-Hsing Lin,^{1,#} Cheng-Tai Lu,¹ Shih-Chieh Yen,¹ Tsu Hsu,¹ Yu-Ling Huang,¹ Jen-Shin Song,¹ Chun-Hwa Chen,¹ Ling-Hui Chou,¹ Kuei-Jung Yen,¹ Ching-Ping Chen,¹ Po-Chu Kuo,¹ Chen-Lung Huang,¹ H. Eugene Liu,² Yu-Sheng Chao,¹ Teng-Kuang Yeh,^{1,*} and Weir-Torn Jiaang^{1,*}

¹Institute of Biotechnology and Pharmaceutical Research, National Health Research Institutes, No. 35, Keyan Rd., Zhunan Town, Miaoli Country 350, Taiwan, R.O.C.

²Graduate Institute of Clinical Medicine, Taipei Medical University, Taipei, Taiwan, R.O.C. Division of Hematology and Oncology, Department of Medicine, Wan Fang Hospital, Taipei Medical University, Taipei, Taiwan, R.O.C.

Chiung-Tong Chen, John T.-A. Hsu and Wen-Hsing Lin contributed equally.

*Corresponding authors

➤ Compound **7h** was assayed against 73 protein kinases at a concentration of 0.1 μ M

Protein kinase inhibition (%) at 100 nM							
FLT3	98	BLK	78	NEK1	23	GSK3A (GSK3 alpha)	2
PDGFRA	98	YES1	72	CSK	23	SGK (SGK1)	2
SRC	97	ABL1	66	RPS6KB1 (p70S6K)	22	RPS6KA5 (MSK1)	0
LYN A	96	KIT	64	RAF1Y340D Y341D	21	ERBB2 (HER2)	0
AURKA	96	PDGFRA V561D	63	TYK2	21	CDC42 BPA (MRCKA)	0
RET	95	MAP2K1 (MEK1)	62	PDGFRA D842V	21	AKT1 (PKB alpha)	0
CSF1R (FMS)	94	IRAK4	61	IKBKE (IKK epsilon)	18	RPS6KA3 (RSK2)	-1
SRC	93	TEK (Tie2)	61	CHEK1 (CHK1)	17	CHEK2 (CHK2)	-3
LCK	92	ABL1 T315I	51	IGF1R	16	MST1R (RON)	-3
PDGFRB	91	PDGFRA T674I	46	AMPK A1/B1/G1	16	JAK2	-3
RET V804L	89	BTK	46	MAPK8 (JNK1)	15	NEK2	-4
FGR	89	FYN	46	MET (cMet)	14	FRAP1 (mTOR)	-7
LYN B	88	HCK	45	MAPK14 (p38 alpha)	10	CLK2	-7
FLT3 D835Y	87	AURKC	45	FGFR1	10	JAK1	-8
RET Y791F	86	GSK3B	44	PLK1	9	SGKL (SGK3)	-8
KDR (VEGFR2)	85	FLT1 (VEGFR1)	44	RPS6KA2 (RSK3)	7	PIM1	-11
AURKB	85	MAP2K1 (MEK1)	41	SGK2	6	AXL	-16
NTRK1 (TRKA)	82	BRAF	36	CLK1	5		
FLT4 (VEGFR3)	80	TYRO3 (RSE)	28	CDK2/cyclin A	4		

STANDARD 1H OBSERVE

exp4 std1h

SAMPLE
date Jul 4 2011
solvent DMSO
file exp
ACQUISITION
sfrq 299.994
t1 1.000
at 1.995
np 17866
sw 4500.3
fb 2600
ls 6
tpwr 56
pw 7.9
d1 1.000
tof 0
nt 1000
ct 40
a1ock n
gain not used
FLAGS
i1 n
in n
dp Y
DISPLAY
sp -402.9
wp 4198.7
vs 894
sc 9
wc 250
hzmm 16.80
is 110.86
rfl 1453.6
rfa 759.0
th 4
ins 100.000
nm cdc ph

DEC. & VT
dfrq 299.994
dn H1
dprw 30
dof 0
dm nnn
dmc c
dmc 200
f0 0.10
proc
fn not used
ft
werr
wexp
wnt

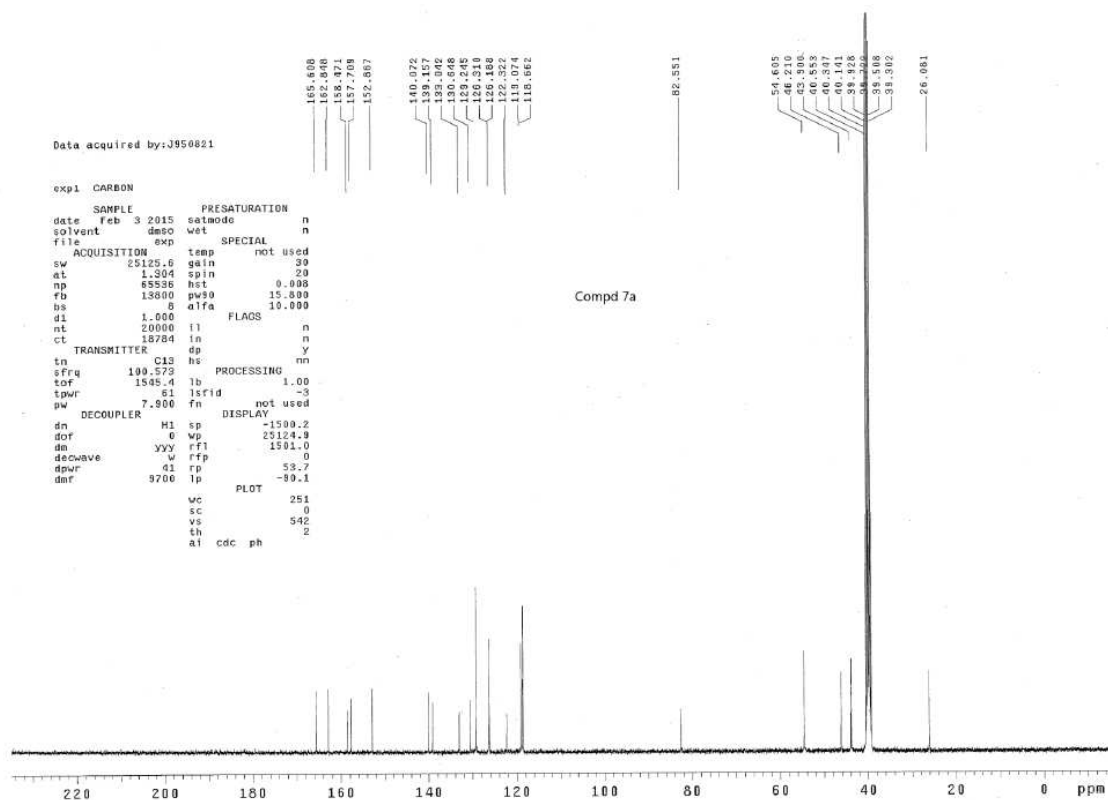
Compd 7a

8.768
8.666
7.644
7.486
7.482
7.309
7.272
7.256
6.399
6.372
6.316
6.053
3.503
3.492
2.418
2.413
2.222

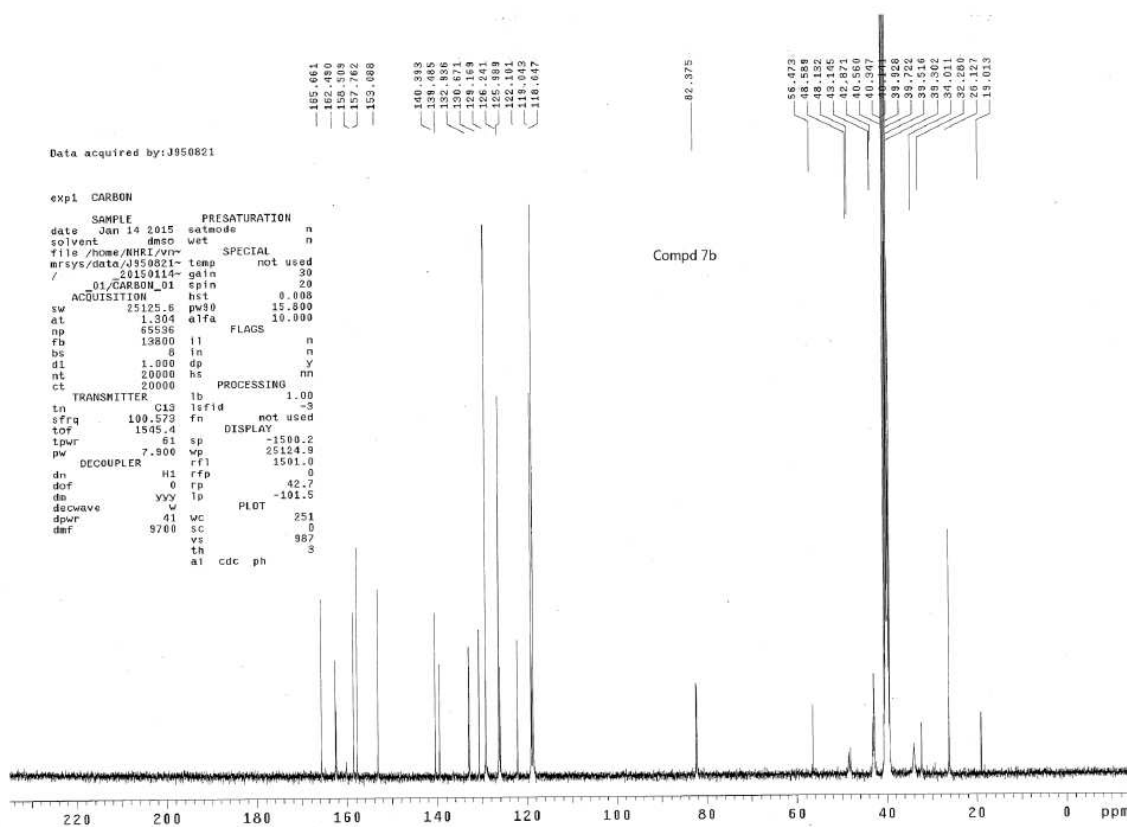
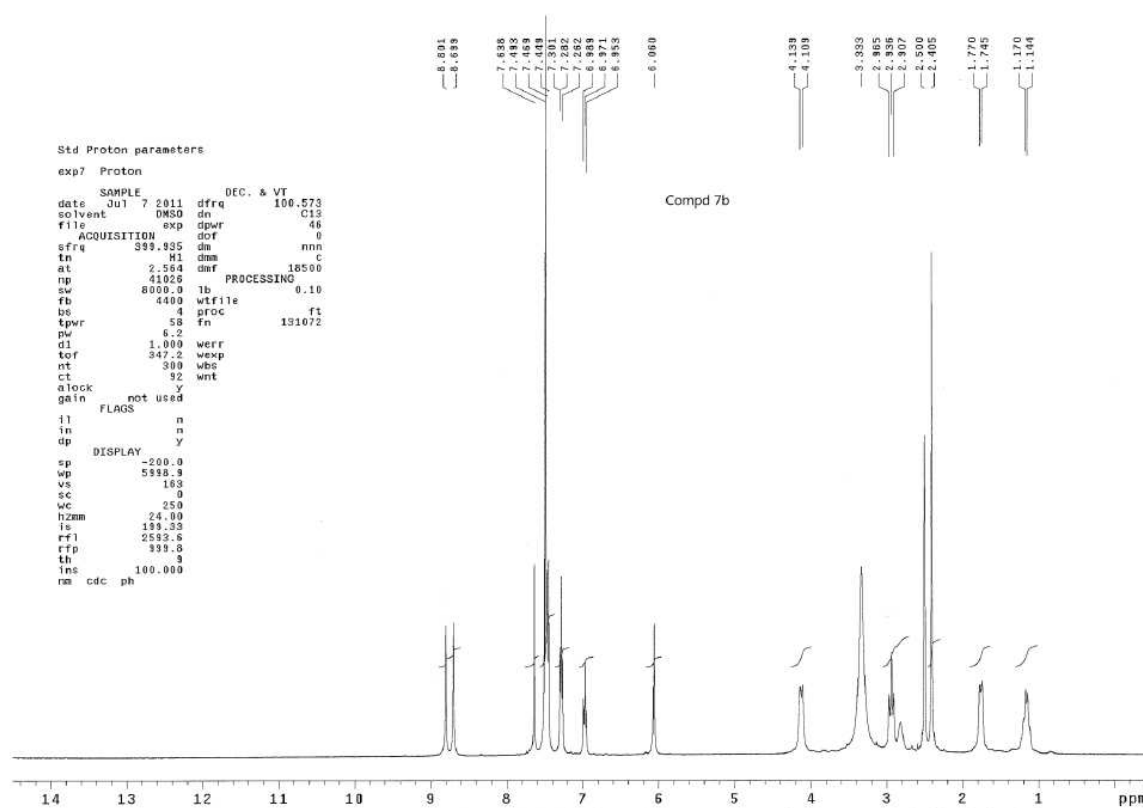
11
9
8
7
6
5
4
3
2
1
0

12 11 10 9 8 7 6 5 4 3 2 1 0 ppm

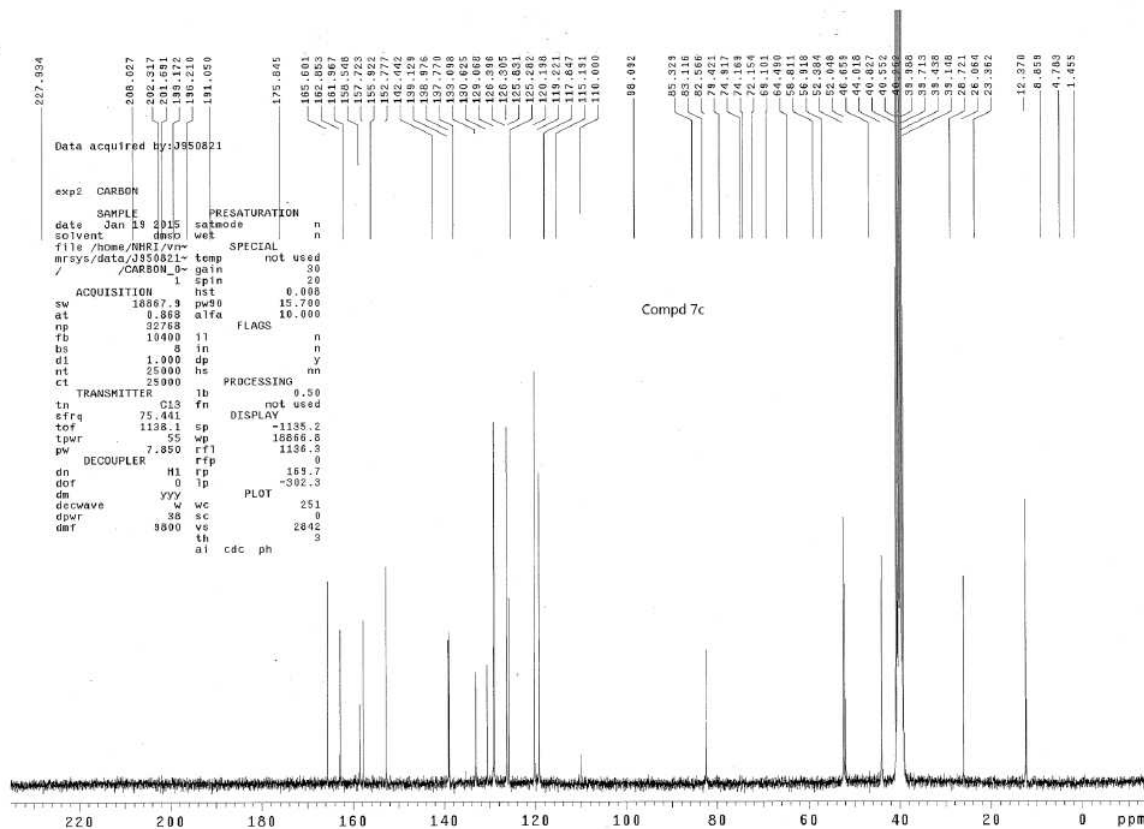
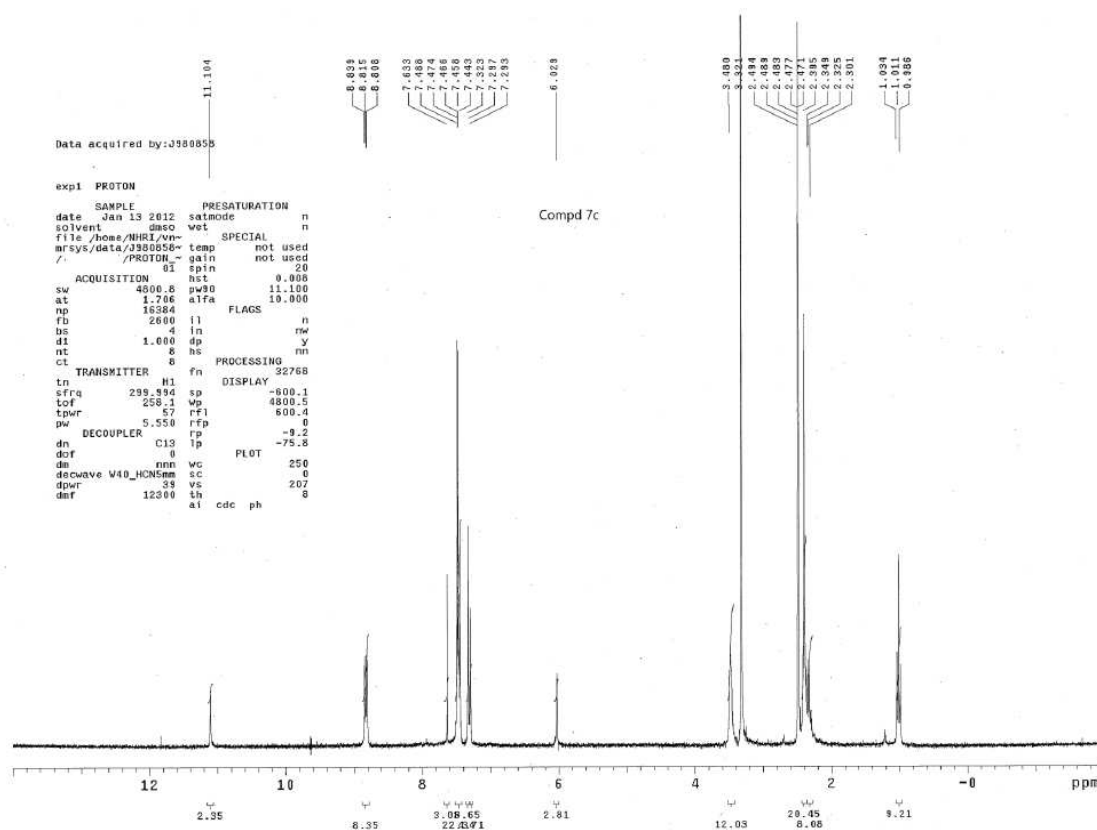
2.55
3.53
3.81
7.65
3.60
14.93
12.50
24.92



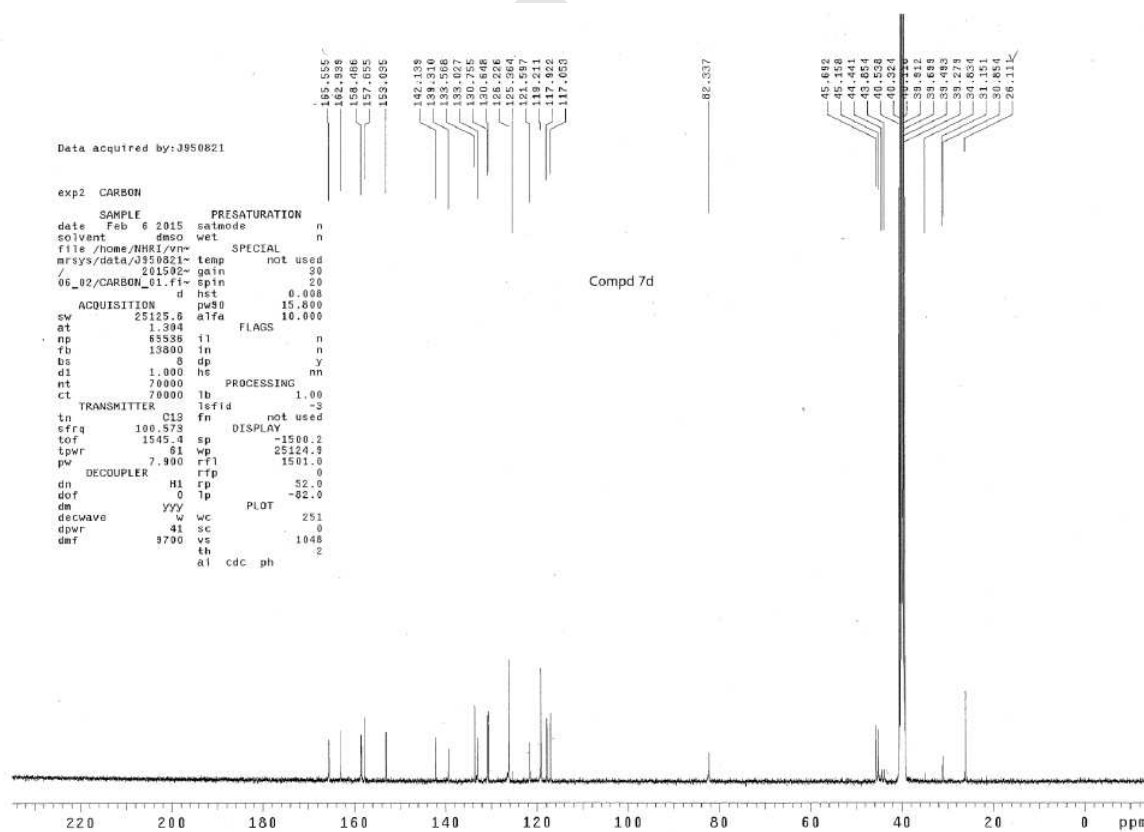
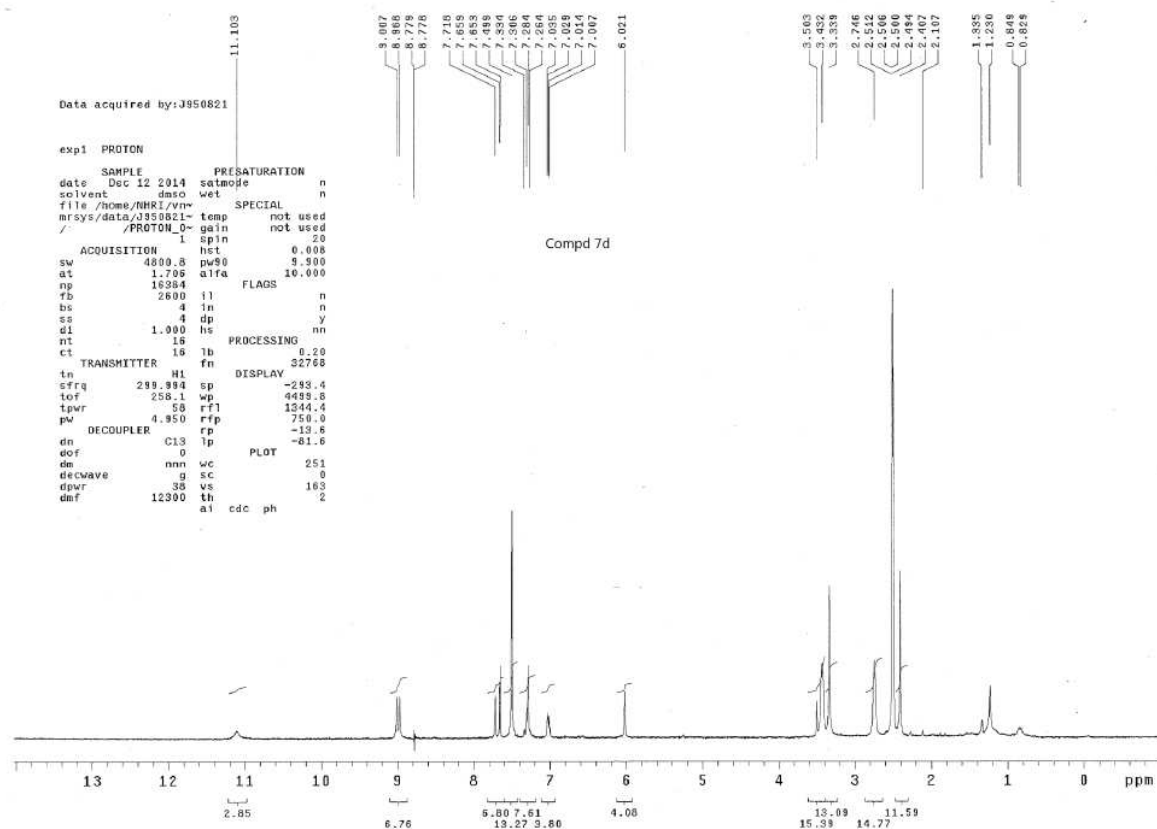
Compound 7b:



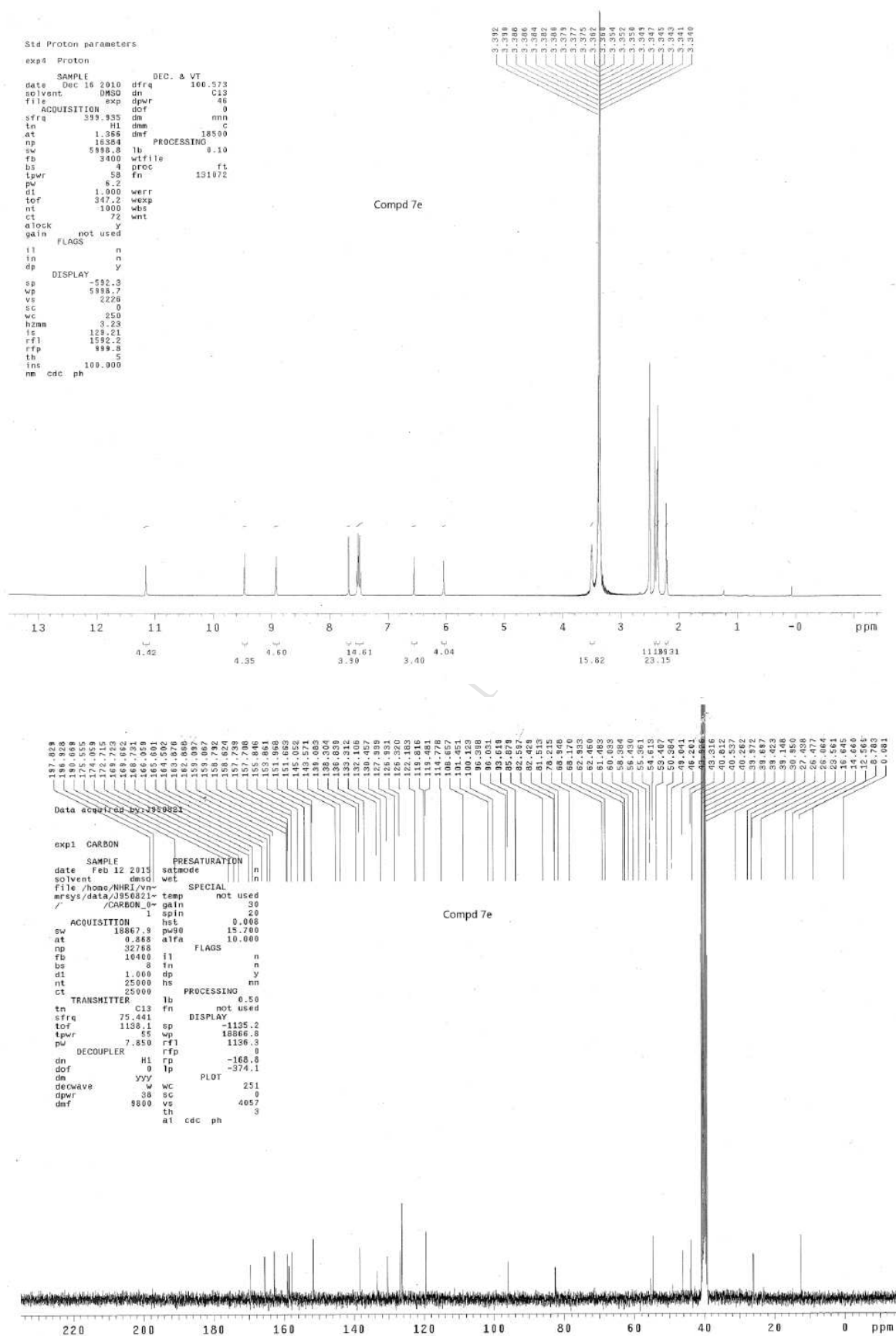
Compound 7c:



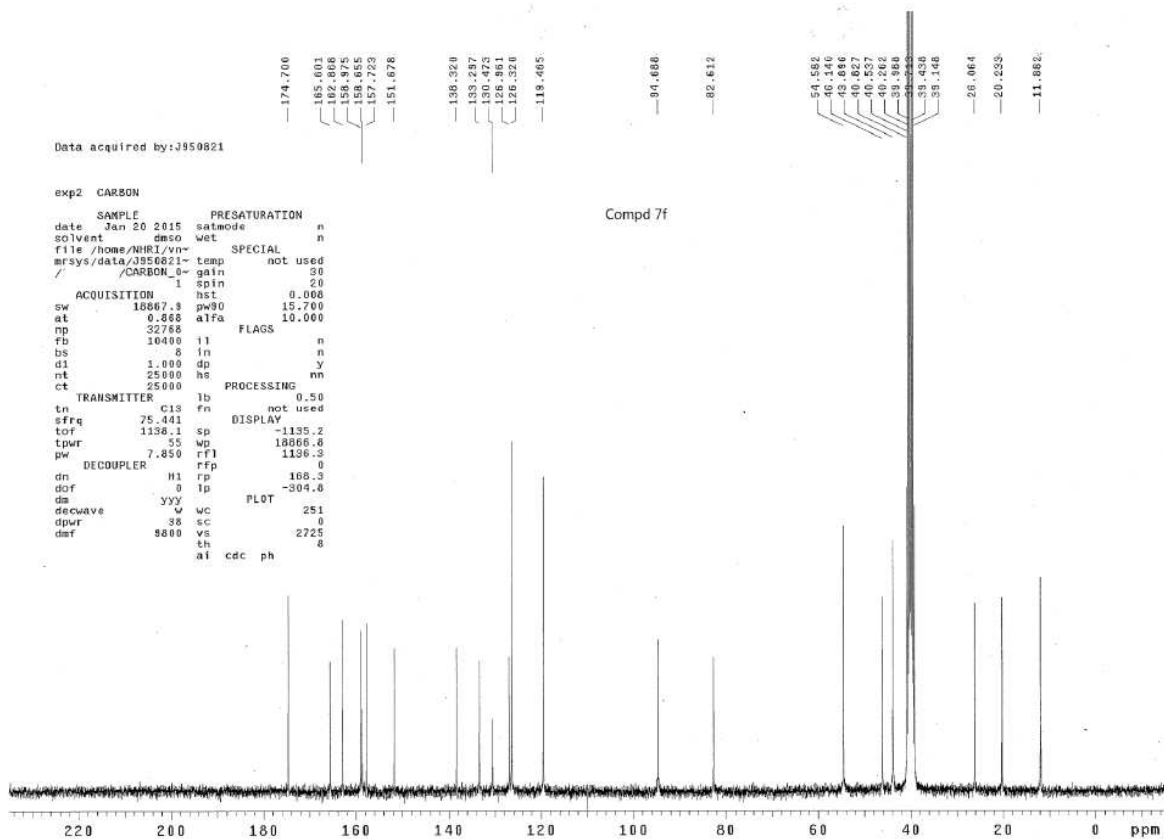
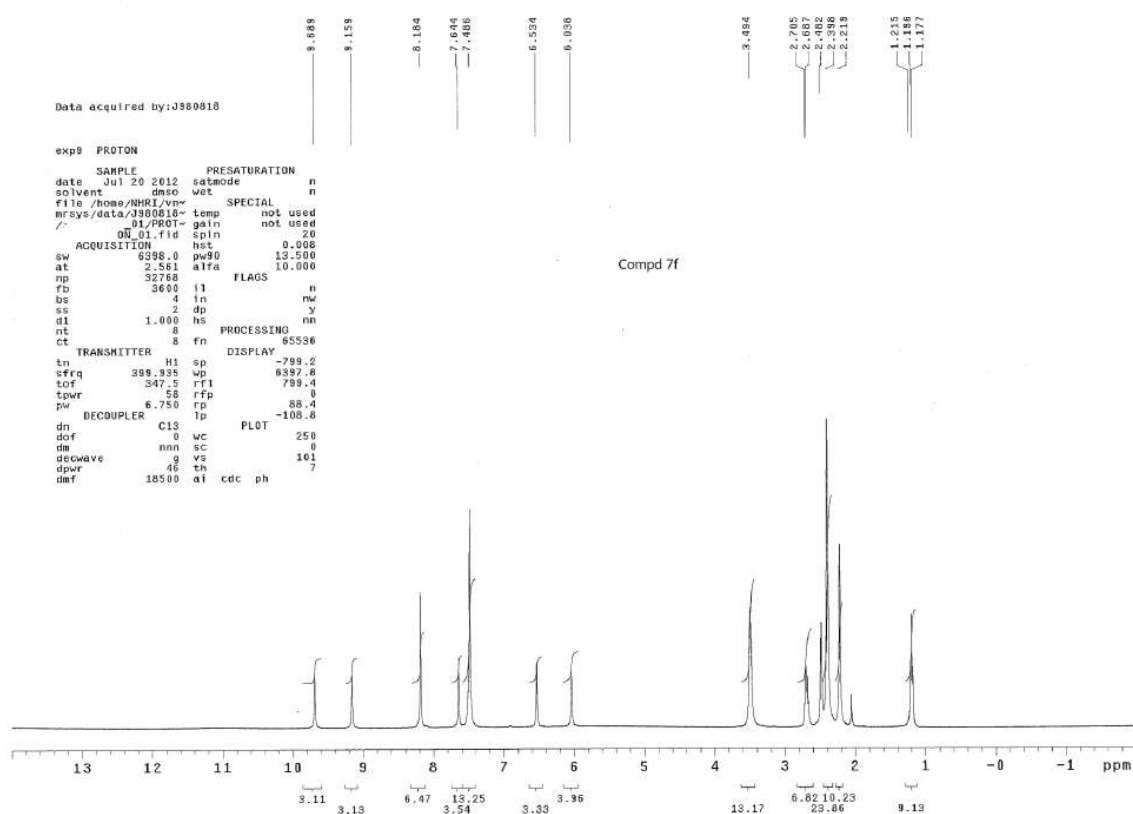
Compound 7d:



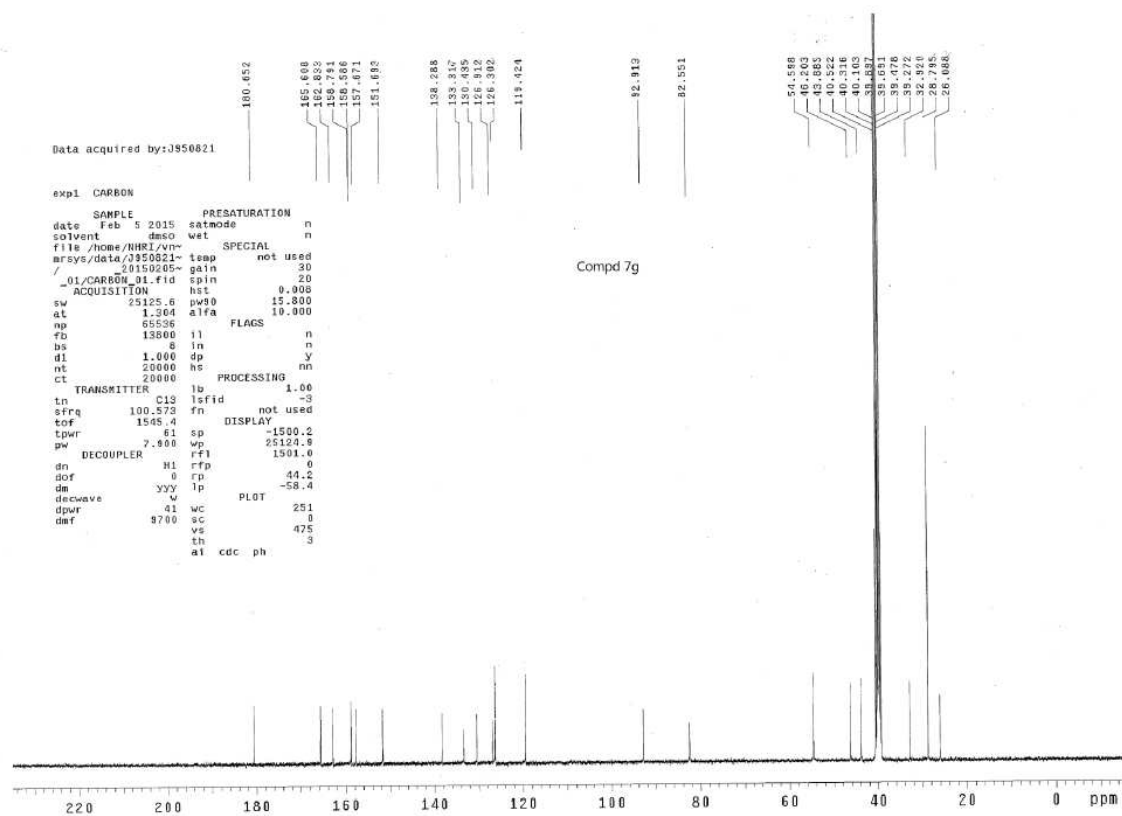
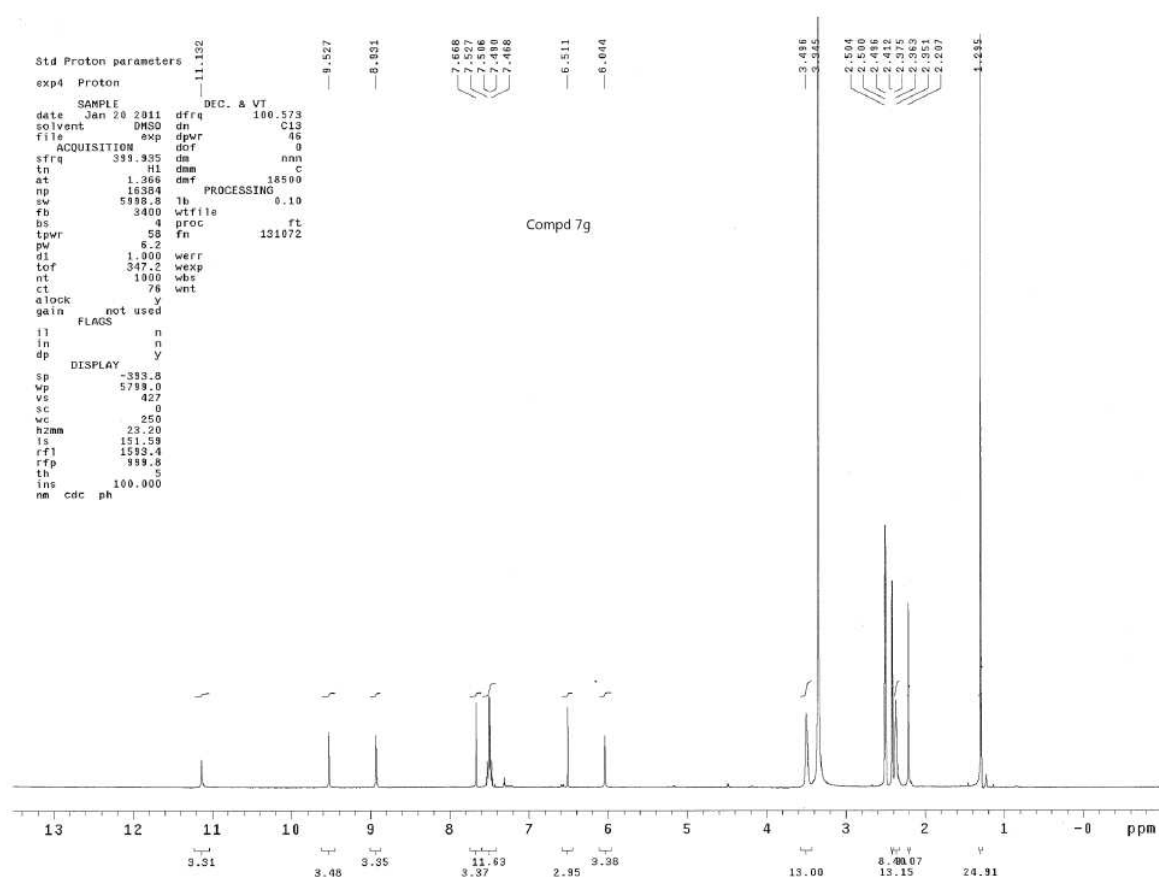
Compound 7e:



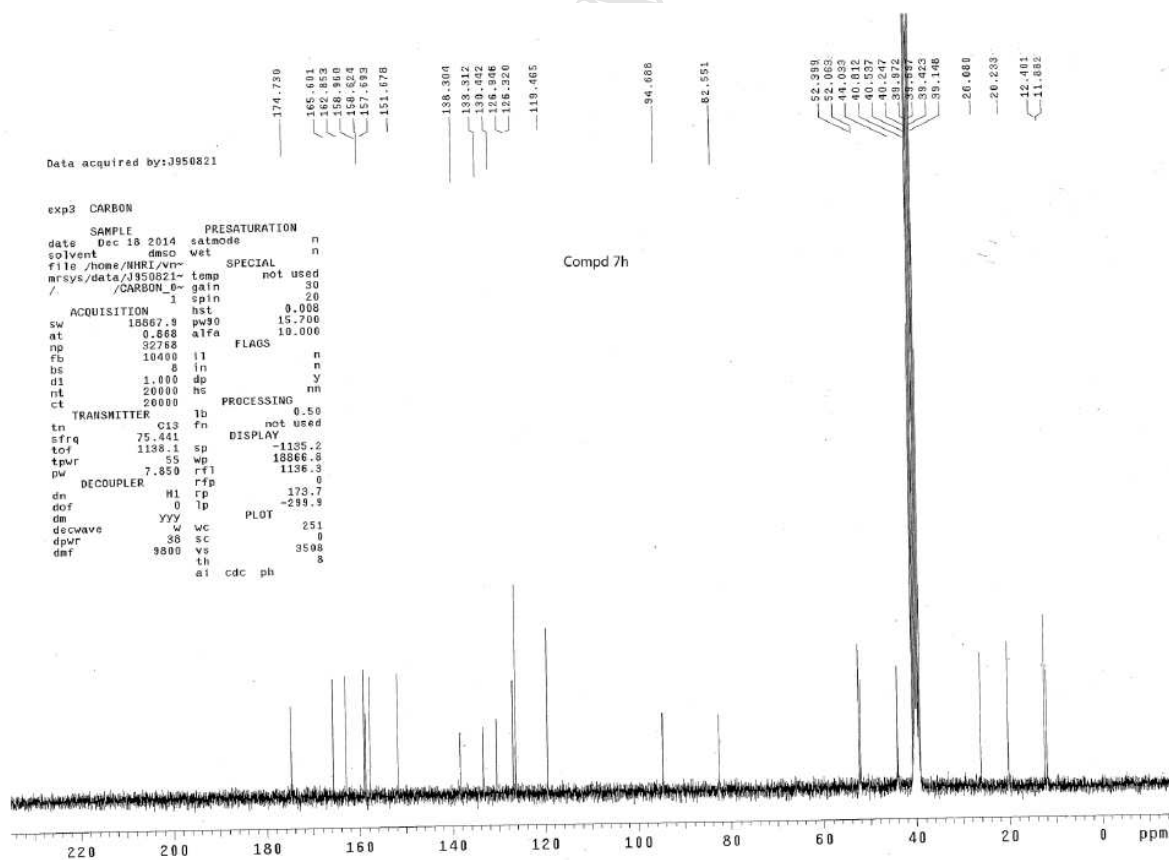
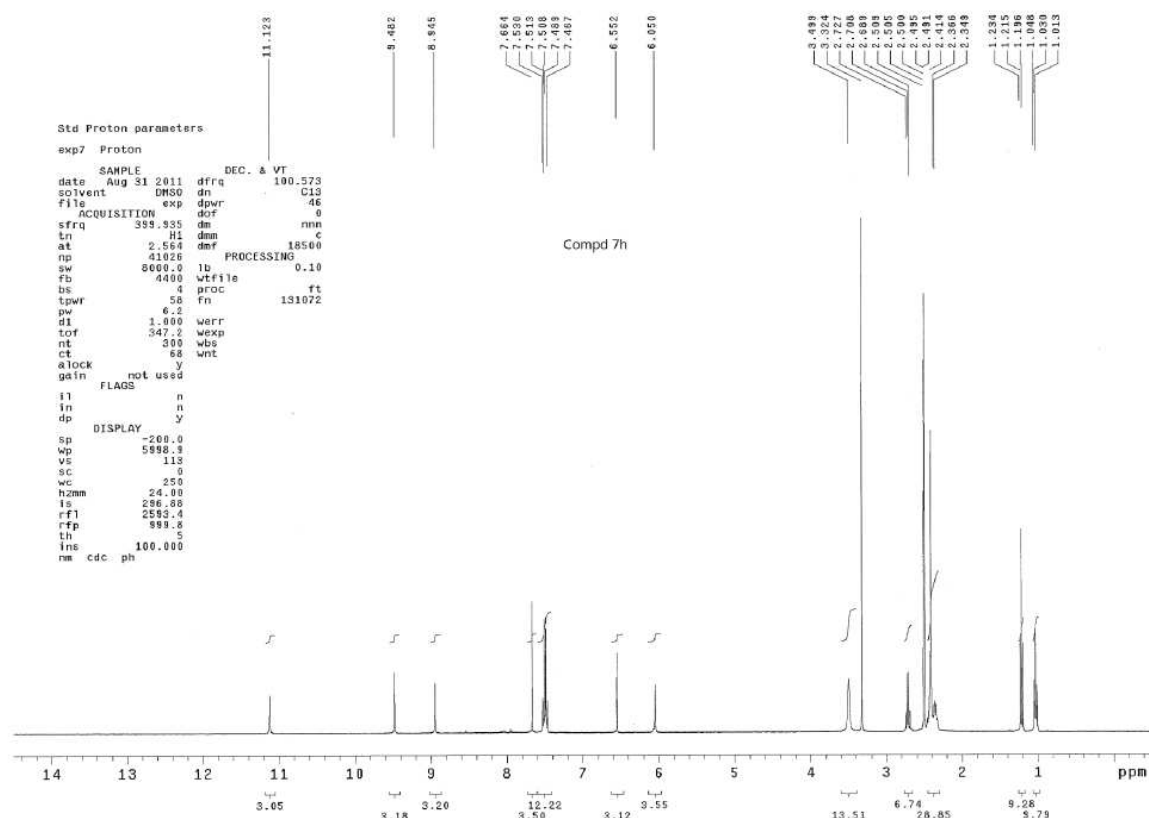
Compound 7f:



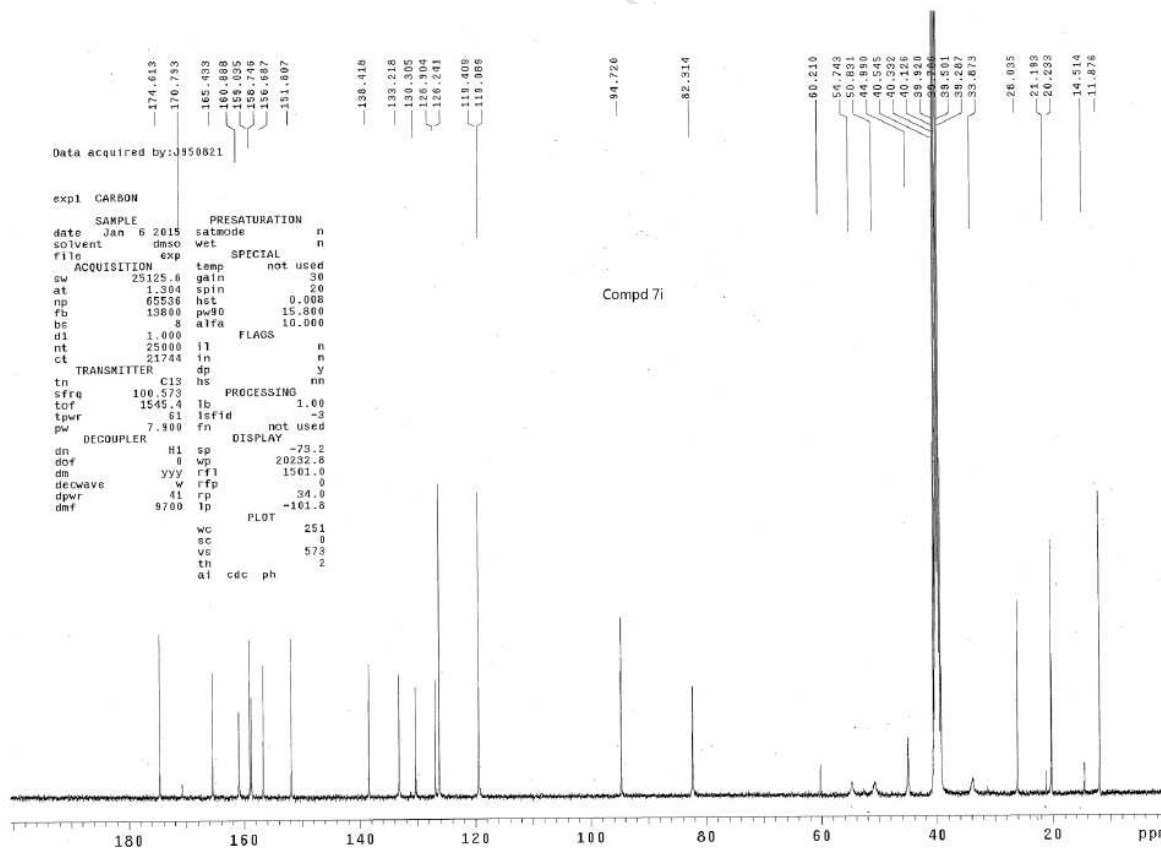
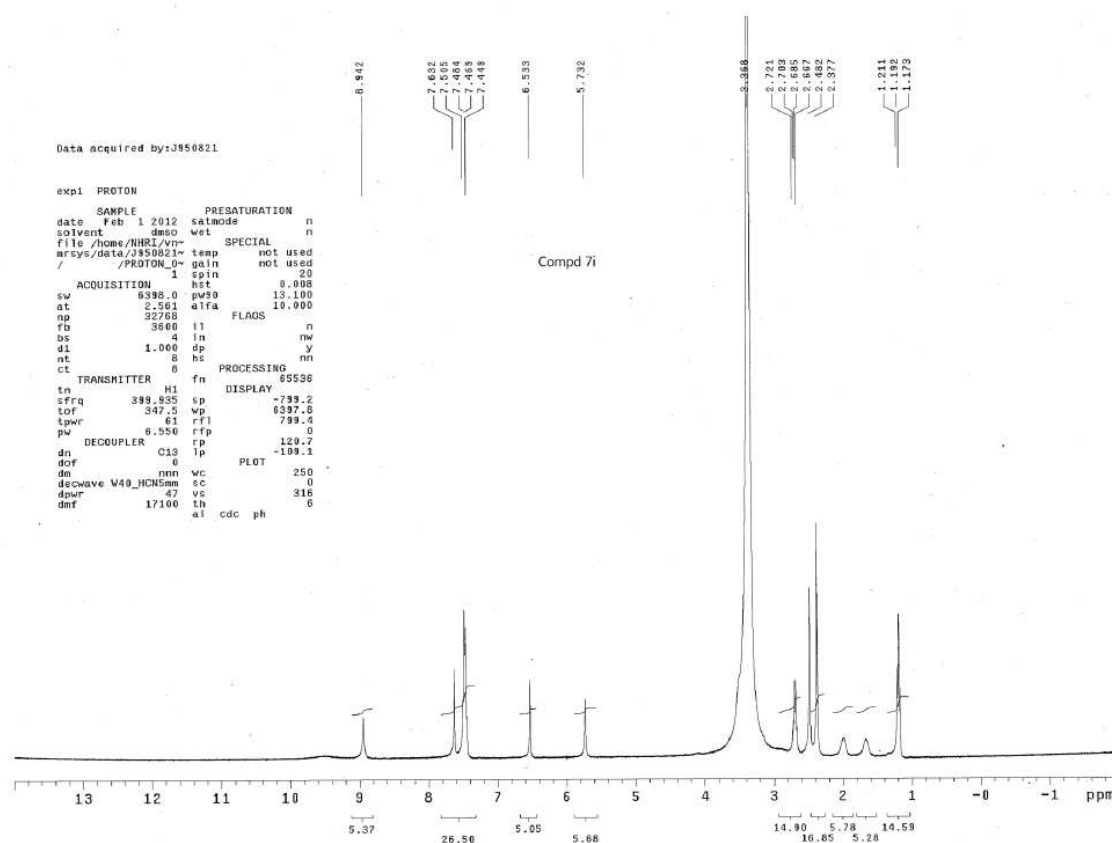
Compound 7g:



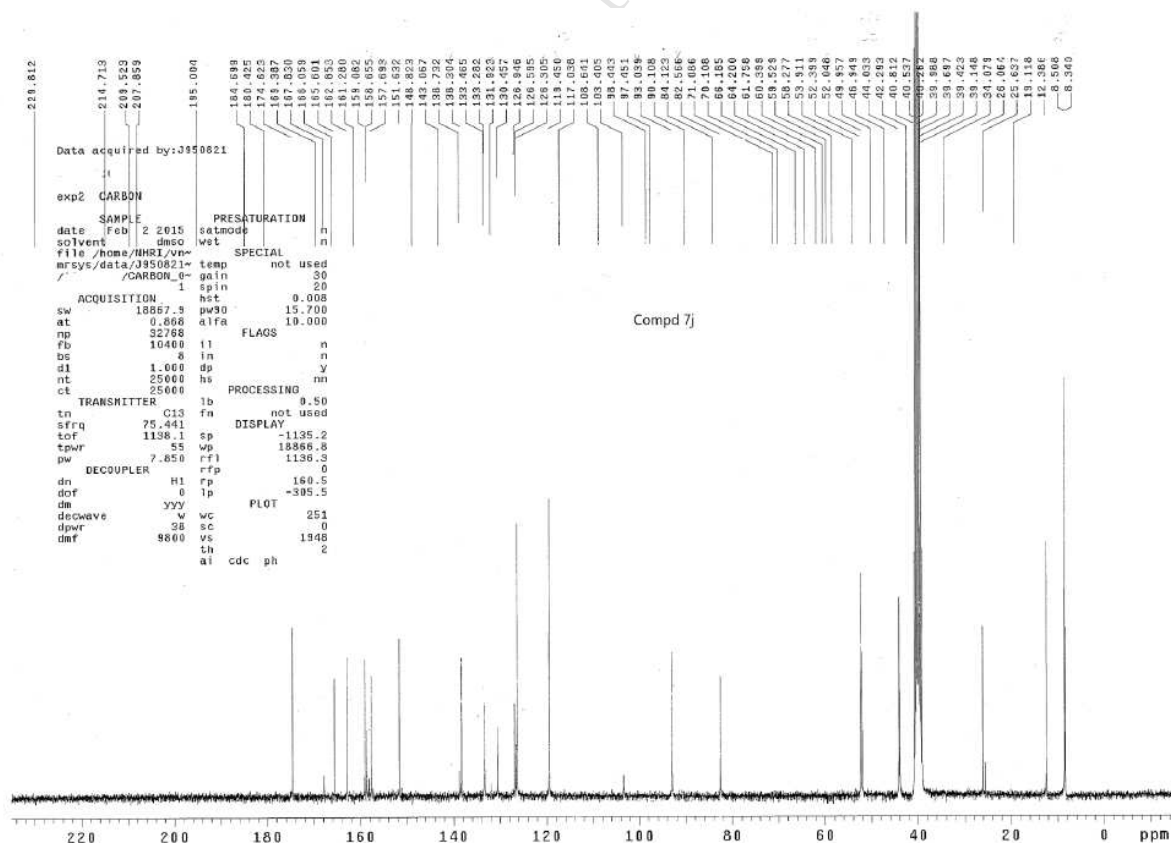
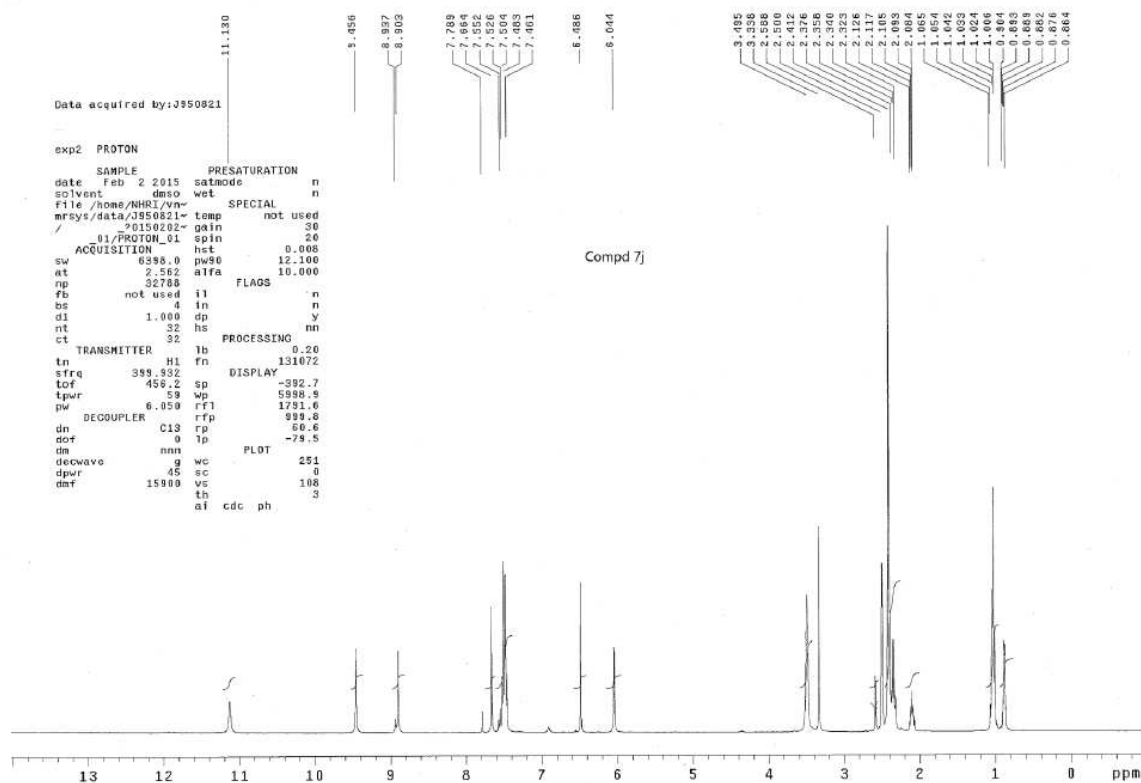
Compound 7h:



Compound 7i:



Compound 7j:



Compound 8:

